

NBER WORKING PAPER SERIES

SOCIAL INTERACTIONS IN PANDEMICS:
FEAR, ALTRUISM, AND RECIPROCITY

Laura Alfaro
Ester Faia
Nora Lamersdorf
Farzad Saidi

Working Paper 27134
<http://www.nber.org/papers/w27134>

NATIONAL BUREAU OF ECONOMIC RESEARCH
1050 Massachusetts Avenue
Cambridge, MA 02138
May 2020

We thank John Cochrane, Pietro Garibaldi, Francesco Lippi, Maximilian Mayer, Dirk Niepelt, Vincenzo Pezone, Mathias Trabandt and Venky Venkateswaran, as well as various seminar participants for their comments and suggestions. All errors are our own responsibility. The views expressed herein are those of the authors and do not necessarily reflect the views of the National Bureau of Economic Research.

NBER working papers are circulated for discussion and comment purposes. They have not been peer-reviewed or been subject to the review by the NBER Board of Directors that accompanies official NBER publications.

© 2020 by Laura Alfaro, Ester Faia, Nora Lamersdorf, and Farzad Saidi. All rights reserved. Short sections of text, not to exceed two paragraphs, may be quoted without explicit permission provided that full credit, including © notice, is given to the source.

Social Interactions in Pandemics: Fear, Altruism, and Reciprocity
Laura Alfaro, Ester Faia, Nora Lamersdorf, and Farzad Saidi
NBER Working Paper No. 27134
May 2020, Revised August 2020
JEL No. D62,D64,D85,D91,I10

ABSTRACT

In SIR models, infection rates are typically exogenous, whereas individuals adjust their behavior in reality. City-level data across the globe suggest that mobility falls in response to fear, proxied by Google searches. Incorporating experimentally validated measures of social preferences at the regional level, we find that stringency measures (conversely their lifting) matter less when individuals are more patient and altruistic, or exhibit less negative reciprocity. To account for these findings, we extend homogeneous and networked SIR models so as to endogenize agents' social-activity intensity. We derive the social planner's problem and draw implications on the optimality of targeted lockdown policies.

Laura Alfaro
Harvard Business School
Morgan Hall 263
Soldiers Field
Boston, MA 02163
and NBER
lalfaro@hbs.edu

Ester Faia
Goethe University Frankfurt
Theodor W. Adorno Platz 3
Frankfurt am Main, 60323
Germany
and CEPR
faia@wiwi.uni-frankfurt.de

Nora Lamersdorf
Goethe University Frankfurt
Theodor W. Adorno Platz 3
Frankfurt am Main, 60323
Germany
lamersdorf@econ.uni-frankfurt.de

Farzad Saidi
Boston University
Questrom School of Business
595 Commonwealth Avenue
Boston, MA 02215
and CEPR
fsaidi@bu.edu

1. Introduction

The onset of the COVID-19 pandemic has sparked a vivid debate on policies aiming to restrict mobility, the role of regional heterogeneity for their effectiveness, and the potential economic cost. As such, economies considering exit strategies from lockdowns seek to implement them in a way that does not endanger a robust recovery from the public health crisis.

As the shape of the recovery is uncertain, a guiding principle for an optimal policy is to consider how the risk of disease has affected agents' behavior, which may not be uniform and could vary widely across regions and individuals. Demand spirals and excessive precautionary behavior, which would impair the recovery, typically result from deep scars.¹ The recovery is unlikely to be fast if agents maintain social-distancing norms due to their risk perceptions.² Beyond that, understanding the endogenous response of social behavior to a pandemic can provide further insights for forecasting how a disease spreads.

In this paper, we show that fear, other-regarding preferences, patience, and interaction in social networks determine individuals' response to the pandemic and, in particular, their mobility choices. We provide evidence from international daily mobility data that fear is negatively associated with walking, driving, and transit at the granular city level. Furthermore, after controlling for fear, any additional effect of (typically country-wide) lockdowns (and the lifting thereof) or other government stringency measures on mobility varies across regions as a function of the latter's average level of patience, altruism, and reciprocity. We then rationalize these findings through the lens of the homogeneous SIR model and an SIR-network model where social-activity intensity depends on individual preferences, namely patience and altruism, and on community traits, namely the matching technology's returns to scale (geographical density) and reciprocity among groups.

For our empirical analysis, we use Apple mobility data, which are obtained from GPS

-
- 1 A recent survey by Bartik et al. (2020) indicates that small businesses are very pessimistic about a possible recovery due to social distancing.
 - 2 A quote from Larry Summers (Fireside Chats with Harvard Faculty on April 14, 2020) highlights this aspect: "You can open up the economy all you want, but when they're hiring refrigerator trucks to deliver dead bodies to transport them to the morgues, not many people are going to go out of their houses...so blaming the economic collapse on the policy, rather than on the problem, is fallacious in the same way that observing that wherever you see a lot of oncologists, you'll tend to see a lot of people dying of cancer and inferring that that means that oncologists kill people."

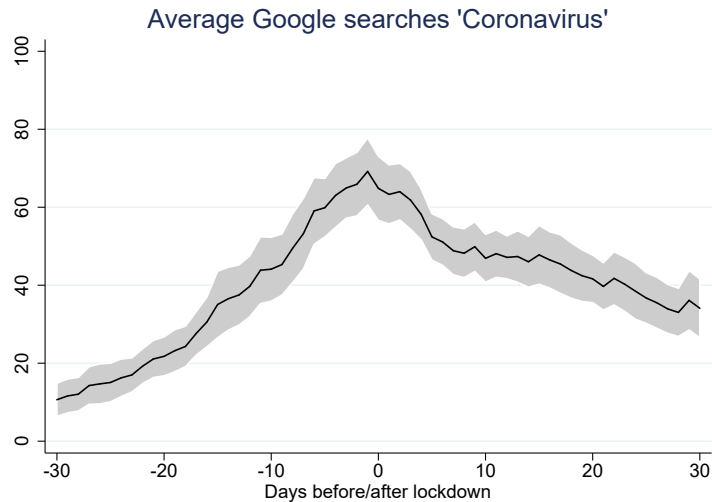


Figure 1
City-level Google Searches around Lockdown Dates across Countries

tracking. These data provide indicators on walking, driving, and transit, are daily, have a long time coverage, and offer city-level granularity across 45 countries (262 cities in 23 countries in our most restrictive sample).

Figure 1 plots the average value of the Google Trends Index for “Coronavirus” in 33 countries (that have lockdown dates) for the period from 30 days before to 30 days after each country’s lockdown.³ Fear, as proxied for by Google searches, increases up to shortly before the country’s lockdown date, drops thereafter, and eventually levels off (around the same level as two weeks prior to the lockdown).

The negative correlation between city-level mobility and risk perceptions, or fear, is robust to controlling for different mitigation policies, which vary across countries (and across states in the US). In fact, we use a sample period that is long enough to comprise both lockdowns and subsequent relaxations, in conjunction with experimentally validated survey measures from the Global Preferences Survey (see Falk et al. (2018)) to explore the interaction of mitigation policies with time and social preferences.

Importantly, these granular data allow us to exploit regional variation, and to test for heterogeneous effects across regions within a country following lockdowns and the lifting thereof as a function of average preferences in these regions. To control for time-varying

³ We use the earliest date for any state-level lockdown in the US.

unobserved heterogeneity at the country level, we incorporate country-month fixed effects. After including the latter and controlling for fear, we find that the impact of stringency policies on mobility is muted in regions in which individuals are more patient, in which they have a higher degree of altruism, and in which they exhibit less negative reciprocity. Additionally, we find that trust, a cultural characteristic placed between pure altruism and reciprocity, also mutes mobility responses to government interventions.⁴ In sum, in regions with such traits, lockdowns are less likely to (additionally) bring down mobility, as it is reduced well before the implementation of any stringency measures, and mobility is less likely to pick up again once any such mitigation policies are relaxed. We also find that transit tends to react more than walking or driving, which is intuitive since the higher density of cities' transportation systems increases infection risk and fear, reflecting general geographical aspects related to cities' density.

Motivated by these findings, we enrich the classic SIR model from epidemiology,⁵ and in particular modify both the homogeneous SIR and the SIR-network model to account for agents' optimizing decisions on social interactions.⁶ In the SIR-network model, we include different groups with varying contact rates (i.e., varying degrees of homophily) and different recovery rates. Within a community hit by COVID-19, age groups are differentially exposed to health risk and depending on the structure of the community, their interaction might be more or less intense. Even more modern variants of this class of models, which account for the heterogeneous topology of contact networks, assume exogenous contact rates – something that is starkly at odds with reality.

Our model lends support to the idea that preference and community traits matter in line with our empirical evidence. We show analytically that susceptible individuals internalize infection risk based on their patience, infected individuals do so based based on their altruism, and the degree of homophily, which dampens negative reciprocity, matters for internalizing risk in SIR networks. The matching technology's returns to scale captures the geography of cities in terms of density of interactions.

4 See Berg et al. (1995), Bohnet and Frey (1999), Andreoni (1989), and Andreoni (1993).

5 SIR stands for “S,” the number of susceptible, “I,” the number of infectious, and “R,” the number of recovered, deceased, or immune individuals.

6 Recently, other papers have included some form of optimizing behavior as well. We review them below.

Simulations which compare our SIR models with the traditional version confirm our conclusions. In particular, simulations of model variants where agents adjust their social activity in response to risk, altruism, and homophily all exhibit a significantly flattened infection curve compared to the traditional SIR model. Altruism also implies that susceptible individuals have to reduce their social interactions by less, as part of the burden of flattening the curve is borne by the infected individuals. A lower degree of homophily in the SIR-network model implies that, for example, younger agents meet older agents more frequently. If they are altruistic, they take into account the lower recovery rates of the older agents and adjust their behavior accordingly. However, old susceptible individuals reduce their social activity relatively more due to their higher health risk.

Despite this adjustment in behaviors, a social planner might want to restrict interactions further due to a static and a dynamic inefficiency of the decentralized outcome. The planner internalizes the effect of individual social activities on the overall congestion of a community, which leads to a static inefficiency. The planner is also aware that her policies can affect the future number of infected individuals, which in turn gives rise to a dynamic inefficiency.⁷ We decompose the two inefficiencies, and show that they depend, among others, on the matching technology's returns to scale, which capture location density and infrastructure. In the SIR-network model, an additional inefficiency arises since the planner also internalizes the differential impact that the activity of each group has on the average infection rate of the others based on their degrees of homophily and, thus, contact rates.

Analytically, we show that lockdown policies targeted toward certain groups are implementable only when identification of infected individuals is possible. Simulations allow us to quantify the optimal lockdown policies. In accordance with our empirical results, we find that the optimal share of locked-down activities is smaller in the presence of altruism. In the SIR-network model, a social planner chooses stricter stringency measures for agents with high social intensity (possibly the younger ones) and when groups exhibit less homophily, as in that case the disease is less likely to be confined to one group, and can spread more easily within communities.

⁷ This is similar to Moser and Yared (2020), in that we highlight a dynamic inefficiency compared to the social planner's commitment.

Relation to Literature. While we devise an application to the pandemic, our theory belongs and contributes to the class of models used to study endogenous network formation. Closest to our model is that by Currarini et al. (2009), who study the formation of links through utility maximization and the emergence of homophily through a biased search and matching process. Much like them, we study endogenous social interaction also in a network context with utility-maximizing agents and a search and matching process. In contrast, homophily in our model, when introduced, is assumed.⁸ However, in addition, our framework features dynamic optimization and studies both the decentralized equilibrium as well as the social planner’s problem.

Our paper also relates to the literature on informal insurance in random and social networks. This literature studies how transfers and obligations translate into global risk sharing (see Ambrus et al. (2014), Bloch et al. (2008), or Bramoullé and Kranton (2007)). As in these models, links, whether random or directed, have utility values, and social interactions are chosen by sharing the infection risk within a community. Our empirical analysis contributes to a burgeoning literature that scrutinizes the development of mobility around the pandemic (see Coven and Gupta (2020), Durante et al. (2020), Glaeser et al. (2020), or Goolsbee and Syverson (2020)). In contrast to these studies, we employ novel data for 299 cities worldwide in conjunction with experimentally validated survey measures that link economic preferences and community structure (e.g., through reciprocity). To the extent that we examine the effect of fear on mobility, our paper also relates to recent surveys documenting how the pandemic affects beliefs and economic expectations (Binder (2020), Fetzer et al. (2020)).

The theoretical literature on the economics of pandemics is already vast. Here we list some of the theoretical contributions that are closer to ours. Atkinson (2020), Alvarez et al. (2020), Gonzalez-Eiras and Niepelt (2020), and Jones et al. (2020) study the social planner’s problem in the traditional SIR framework. Eichenbaum et al. (2020) highlight the health externality.⁹ Garibaldi et al. (2020) and Farboodi et al. (2020) derive an optimizing SIR model, and Keppo et al. (2020) derive a behavioral SIR model. Closest to our model is

⁸ Kossinets and Watts (2009) show that homophily is often also an inherited trait, and that its pervasiveness tends to be an entrenched attribute of communities rather than the result of an explicit choice.

⁹ Relatedly, Hall et al. (2020) measure the cost of the health externality.

that by Garibaldi et al. (2020). However, unlike them, we model the decision problems of both susceptible and infected agents, and incorporate them also in the network structure. Acemoglu et al. (2020) model an SIR network with different age groups where contacts are determined based on a Diamond (1982) style exogenous matching function.

In the epidemiology literature, there is a large number of SIR variants, starting with Kermack and McKendrick (1927) and, more recently, Hethcote (2000), all with exogenous contact rates. In particular, there are SIR-network models with bosonic-type reaction-diffusion processes (see, for instance, Colizza et al. (2007) and Pastor-Satorras and Vespignani (2001a,b)) or activity-driven SIR-network models (see Moinet et al. (2018) and Perra et al. (2012), who also include a fixed risk-perception parameter that induces a decaying process in the infection rate).

2. Empirical Analysis

In the following, we first describe the data that we use in our empirical analysis. After presenting some evidence for the development of mobility around lockdown dates across different cities and countries, we discuss our empirical strategy for uncovering heterogeneous effects in the effectiveness of lockdowns depending on social preferences and the relationship between mobility and fear.

2.1. Data Description

To measure mobility at the country and city level, we use a data set provided by Apple, which stems from direction requests in Apple Maps.¹⁰ Mobility is split into three categories: walking, driving, and transit. The data are at a daily frequency and start in January 2020. They cover 299 cities in 45 countries, of which 111 cities are located in 39 states across the US and Washington DC. Our sample period comprises more than five months in 2020, namely from January 22 to June 30.

To obtain an index reflecting potential fear regarding COVID-19, we use the daily number

¹⁰ See <https://www.apple.com/covid19/mobility>.

of Google searches for the term “Coronavirus” in each country and region, provided by Google Trends.¹¹ For a given time period (in our case, January 22 to June 30), Google Trends assigns to the day with the highest search volume in a given country or region the value 100, and re-scales all other days accordingly. Since this leads to large spikes in the time-series data, we use the natural logarithm of these values for our analysis.

We obtain daily numbers on infections and deaths due to COVID-19 at the country level from Johns Hopkins University.¹² This time series starts on January 22, 2020, determining the beginning of the time span covered in our empirical analysis.

To capture policy responses of governments across the globe, we take two approaches. First, we generate a dummy variable that is one from the first day of an official country-wide (or state-wide) lockdown onward and zero otherwise, and a second dummy that is one from the first day of an official country-wide (or state-wide) lifting of such mitigation policies onward and zero otherwise. For this purpose, we use the country-wide lockdown and lifting dates provided by Wikipedia.¹³ Since in the US policy responses differ across states, we use state-wide lockdown and lifting dates for a given city in the respective state for our city-level regressions. We obtain these data from the National Academy for State Health Policy.¹⁴ Since in some cases the lifting or re-opening started gradually, it may be difficult to determine a unique starting date. To this end, we cross-validate these dates with a list of re-opening dates provided by the New York Times.¹⁵ In case the start dates of the lifting period differ, we use the earlier date to generate our dummy variable.

Relatedly, lockdown measures and the lifting thereof may also vary widely in their intensity across countries or states. For this reason, we use as an alternative measure the so-called stringency index, between 0 and 1, at the country-day level from the Oxford COVID-19 Government Response Tracker (OxCGRT), which is available from January 1, 2020 onward.

11 See <https://trends.google.com/trends/?geo=US>.

12 See https://github.com/CSSEGISandData/COVID-19/tree/master/csse_covid_19_data/csse_covid_19_time_series.

13 See https://en.wikipedia.org/wiki/COVID-19_pandemic_lockdowns.

14 See <https://www.nashp.org/governors-prioritize-health-for-all>.

15 See <https://www.nytimes.com/article/coronavirus-timeline.html>.

This index combines several different policy responses governments have taken, and aggregates them into a single measure that is comparable across countries.¹⁶

To analyze whether the effect of government responses on mobility depends on country- or region-specific economic preferences, we use a set of variables from the Global Preferences Survey.¹⁷ This globally representative data set includes responses regarding time, risk, and social preferences for a large number (80,000) of individuals for all countries in our sample. In particular, this data set provides experimentally validated measures of altruism, patience, trust, and reciprocity. These variables map to parameters of our theoretical model and, thus, enable us to test for heterogeneous effects in our empirical analysis.

As pointed out by Falk et al. (2018), economic preferences tend to differ significantly within countries. Therefore, we use their data set on individual, rather than country-level, survey responses, and compute for each variable the average value at the level of the regions corresponding to the cities included in the Apple Mobility data.

We present summary statistics in Table 2. In particular, the statistics in the first four columns pertain to the country-day level ct , whereas those in the last four columns are at the more granular city-day level it for the mobility outcomes, and at the region-day level gt for all remaining variables. Mirroring our regression sample in the respective tables, the sample in the last four columns is furthermore limited to countries with at least two cities in different regions. In this manner, we are left with 262 (out of a total of 299) cities, of which 111 are in the US (see Table 1).

The Google Trends Index for the search term “Coronavirus” exhibits similar average values both at the country and at the regional level. We include summary statistics for the variables we employ from the Global Preferences Survey (Falk et al. (2018)), which are available at the regional level. While altruism and patience are positively correlated (with a correlation coefficient of 0.40), both are negatively correlated with the proxy for negative reciprocity (-0.05 and -0.06). Altruism and patience are highly positively correlated with trust (with

¹⁶ For more information and the current version of a working paper describing the approach, see <https://www.bsg.ox.ac.uk/research/research-projects/coronavirus-government-response-tracker>.

¹⁷ For more information on this survey, see <https://www.briq-institute.org/global-preferences/home> and also Falk et al. (2016, 2018).

correlation coefficients of 0.48 and 0.57, respectively), while the correlation with negative reciprocity is weaker (0.07).

2.2. Motivating Evidence

We start by presenting evidence that motivates our investigation of the effect of fear on mobility, and the role of other-regarding preferences for the effectiveness of lockdowns. In Figure 2, we plot average city-level values for the walking, driving, and transit indices, based on the Apple Mobility data, around lockdown and lifting dates (in our regression sample limited to countries with at least two cities in different regions), which are determined at the state level in the US and at the country level in all other countries. For the figures, we use thirty days before any lockdown measures and after the lifting thereof, thereby focusing on countries (US states) that have experienced both until the end of our sample (June 30, 2020). The interim period is rescaled to represent each country's (US state's) timeline.

The three figures in the left panel plot mobility over time for the US vs. the rest of the world (RoW). Mobility is drastically reduced well in advance of any lockdown, drops more outside of the US, but picks up both in the US and elsewhere even before any lifting of mitigation policies. In the right panel, we zoom in on transit as a mobility outcome that is most likely to generate negative externalities during the pandemic (as opposed to driving, possibly in isolation, and walking in less densely populated areas). During transit infection risk is higher, particularly so in dense cities with ramified transportation systems (this aspect will be captured in the model by the returns to scale of the matching function). We plot these time series for regions in which individuals report to exhibit different average levels of patience, negative reciprocity, altruism, and trust (based on the Global Preferences Survey).

The following stylized facts emerge. The pre-lockdown reduction in mobility is more emphasized in regions in which individuals are more patient, exhibit less negative reciprocity, are more altruistic, and more trusting, which we approximate by sorting regions into the top vs. bottom quarter in terms of $Patience_g$, $Neg. reciprocity_g$, $Altruism_g$, and $Trust_g$.

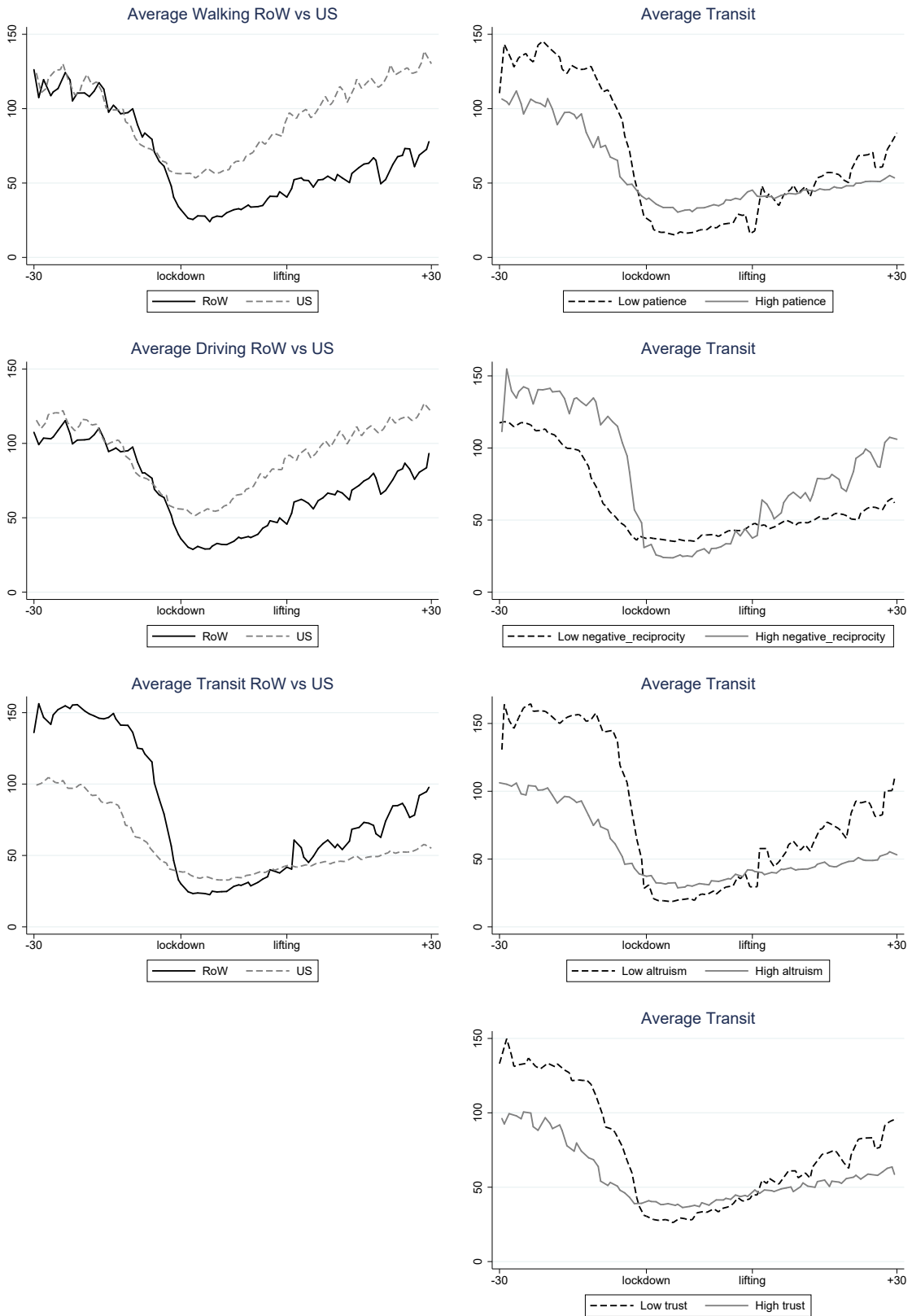


Figure 2
Mobility around Global Lockdown and Lifting Dates

Interestingly, individuals in these regions are also less likely to increase their mobility again once the mitigation measures are relaxed.

We next discuss our empirical strategy for formally testing these relationships in a regression framework.

2.3. Empirical Specification

To assess the relationship between government responses and mobility across different cities worldwide, controlling for fear, we estimate the following regression specification at the city-day level it , with each city i being located in region g of country c :

$$\ln(\text{Mobility})_{it} = \beta_1 \ln(\text{Corona } ST)_{ct-1} + \beta_2 \text{Lockdown}_{ct} + \beta_3 \text{Lifting}_{ct} + \beta_4 \mathbf{X}_{ct} + \mu_i + \delta_t + \epsilon_{it}, \quad (1)$$

where the dependent variable is the natural logarithm of Apple Mobility’s walking, driving, or transit index for city i at date t ; $\text{Corona } ST_{ct-1}$ is the Google Trends Index for the search term “Coronavirus” in country c at date $t - 1$; Lockdown_{ct} is an indicator variable for the entire post-period following a lockdown in country c (or state/region g for the US), and Lifting_{ct} is an indicator variable for the period following the first date which marks the lifting of restrictions in country c (or state/region g for the US); \mathbf{X}_{ct} denotes control variables at the country-day level; and μ_i and δ_t denote city and day fixed effects, respectively. Standard errors are double-clustered at the city and day levels.

In contrasting between fear, as captured by β_1 , and government (typically country-level) responses, as captured by β_2 and β_3 , we can further refine our measure of the former by using the regional average of the Google Trends Index for “Coronavirus.” This effectively enables us to exploit variation in fear across different regions in the same country, in which all regions typically face the same mitigation policies (the US is the only notable exception in our data).

For this reason, when we use regional variation in $\text{Corona } ST_{gt}$, we limit the sample to countries c with at least two cities i in different regions g . This, in turn, allows us to include country-month fixed effects, thereby estimating the effect of lockdowns, or other government measures, while holding constant all remaining sources of unobserved heterogeneity at the

country level in a given month. In this setting, we can then test for heterogeneous effects across regions within a country. In particular, we hypothesize that regions with a certain preference, $Preference_g$, such as greater altruism or patience (see right panel of Figure 2), reduce their mobility more preceding any government responses, thereby muting any additional effect of $Lockdown_{ct}$ on mobility. Similarly, we hypothesize that such regions increase their mobility less following the lifting of mitigation policies, captured by $Lifting_{ct}$. To test this, we estimate the following regression specification:

$$\begin{aligned} \ln(Mobility)_{it} = & \beta_1 \ln(Corona\ ST)_{gt-1} + \beta_2 Lockdown_{ct} + \beta_3 Lockdown_{ct} \times Preference_g \\ & \beta_4 Lifting_{ct} + \beta_5 Lifting_{ct} \times Preference_g + \beta_6 \mathbf{X}_{ct} \\ & + \mu_i + \delta_t + \theta_{cm(t)} + \epsilon_{it}, \end{aligned} \quad (2)$$

where $Corona\ ST_{gt-1}$ is the Google Trends Index for the search term ‘‘Coronavirus’’ in region g at date $t - 1$; $Preference_g$ is the average value of altruism, patience, negative reciprocity, or trust in region g (as reported by Falk et al. (2018)); and $\theta_{cm(t)}$ denotes country-month fixed effects ($m(t)$ is the month for a given day t).

Finally, by testing for the heterogeneous effect of, for instance, altruism at the regional level following lockdowns within countries, we mitigate the risk of picking up potential reverse causality. This is because government policies are typically put in place with the entire, or rather average, population in mind.

2.4. Results

In the first three columns of Table 3, we estimate (1), and use as dependent variables the Apple mobility indices for walking, driving, and transit (the latter variable being available only for a subset of our regression sample). In addition, we control for the lagged number of deaths and infection cases in a given country. Importantly, we use country-level variation in $Corona\ ST_{ct}$, and see that fear, as proxied for by the latter variable, is negatively associated with mobility, above and beyond any government responses. Furthermore, mobility reductions following lockdowns are at least partially reversed after the latter are lifted.

These insights hold up to using regional variation in *Corona ST_{gt}* in the last three columns of Table 1. Fear has a robust negative association with mobility that extends beyond any government response. The effect of fear is not only statistically but also economically significant. As can be seen in Figure 1, Google searches for “Coronavirus” have rapidly increased during the run-up period to a lockdown. For instance, observing a 25% increase in the respective Google Trends index would not be out of the ordinary, which would, in turn, be associated with at least $25\% \times 0.062 = 1.6\%$, $25\% \times 0.072 = 1.8\%$, and $25\% \times 0.094 = 2.4\%$ less walking, driving, and transit, respectively, in cities.

We next test for heterogeneous effects across regions within a country, as a function of average preferences in said regions. In particular, we hypothesize that regions in which individuals report to be more patient should exhibit a muted response to lockdowns as patient agents are more likely to postpone any acts of mobility for the sake of internalizing any externalities on susceptible agents. We also test for analogous effects following the initial lifting of previous lockdown decisions, i.e., whether regions with more patient individuals are subsequently less likely to pick up their mobility. Similarly, we would expect agents with other-regarding preferences, especially altruistic agents, to behave this way. Due to the empirically high correlation between the two latter measures and trust, we also differentiate regions by their average level of trust. Finally, agents that exhibit negative reciprocity are more prone to mimic any acts of mobility out of inequity aversion, so the negative effect of lockdowns and the positive effect of lifting the latter on city-level mobility should be more emphasized for regions in which individuals exhibit greater negative reciprocity.¹⁸

These preference parameters are captured by the respective variables from the Global Preferences Survey and incorporated in regression specification (2). In Tables 4, 5, 6, and 7, we use interactions of *Lockdown_{ct}* and *Lifting_{ct}* with, respectively, *Patience_g*, *Neg. reciprocity_g*, *Altruism_g*, and *Trust_g*.

In the first three columns of Table 4, we find that in regions which exhibit greater patience, the effect of lockdowns on mobility is reduced significantly across the board. Analogously,

¹⁸ As social preferences can be endogenous to certain characteristics of the economy, they may capture specific features of local economies that are not necessarily highly correlated with more aggregate (country-wide) characteristics, which are in turn captured by country-month fixed effects.

any increase in recorded outside activities following the lifting of mitigation policies, such as lockdowns, is dampened in regions with more patient individuals. This is consistent with our evidence in the right panel of Figure 2: lockdowns reduce mobility primarily in regions with less patient individuals who, in turn, exhibit less self-control and refrain less from social activities following an initial lifting of mitigation policies.

Government responses are not uniform, and a simple dummy variable may mask important underlying heterogeneity. For instance, to determine $Lifting_{ct}$, we use the very first date which marks the lifting of restrictions, even when followed by further relaxations thereafter. To this end, we replace the dummy variables $Lockdown_{ct}$ and $Lifting_{ct}$ by a continuous variable, $Stringency\ index_{ct}$, which is an index $\in [0, 1]$ (taken from the Oxford COVID-19 Government Response Tracker) reflecting the different policy responses that governments have taken. Lockdown periods are associated with high values of $Stringency\ index_{ct}$, and the relaxation of such mitigation policies leads to a drop in $Stringency\ index_{ct}$.

The estimates on the respective coefficient in the last three columns of Table 4 are statistically significant at the 1% level throughout, and appear to partially explain some of the effect of fear. Importantly, the interaction effect with $Patience_g$ is positive and significant at the 1% level, which is consistent with our estimates in the first three columns: patience dampens both the drop in mobility following more stringent mitigation policies and the increase in mobility after lifting any such restrictions.

In columns 1 to 3 of Table 5, in line with the idea that individuals that exhibit greater negative reciprocity are less prone to internalize externalities by reducing their mobility, we find that lockdowns are effective in imposing such behavior: the coefficient on $Lockdown_{ct} \times Neg.\ reciprocity_g$ is negative for walking, driving, and transit. Analogously, the coefficient on the interaction with $Lifting_{ct}$ is positive (and always statistically significant at the 1% level). The respective results are qualitatively similar (albeit not statistically significant) for driving and transit when replacing $Lockdown_{ct}$ by $Stringency\ index_{ct}$ (in columns 5 and 6).

Furthermore, the effect of lockdowns on (lower) mobility is significantly reduced in more altruistic regions (see columns 1 to 3 in Table 6). This is in line with altruistic agents' willingness to internalize externalities affecting susceptible agents by reducing their mobility.

As a consequence, lockdowns have only a limited effect on mobility above and beyond fear, the influence of which we capture again through *Corona* ST_{gt-1} . Analogously, altruistic agents are less likely to increase their mobility following the lifting of mitigation policies. The results are qualitatively similar but weaker when using the stringency index in the last three columns.

Finally, we find similar effects when using $Trust_g$, which has been documented, and we confirm, to be highly correlated with altruism and patience. In Table 7, we find – throughout all specifications – that regions that exhibit greater trust react less to government mitigation policies, irrespective of how they are measured, and the relaxation thereof. As mentioned previously, conceptually trust falls between altruism and reciprocity and, thus, constitutes an important cultural trait to control for. In the model, we will use warm-glow preferences as a general formalization of elements that are common to altruism and trust.

3. Limitations of SIR and SIR-Network Models

Motivated by our empirical findings, we formulate an SIR model that accounts for agents’ optimizing behavior with respect to the intensity of their social activity. In the basic homogeneous SIR model (see Kermack and McKendrick (1927) or Hethcote (2000) more recently), there are three groups of agents: susceptible (S), infected (I), and recovered (R) ones. The number of susceptible decreases as they are infected. At the same time, the number of infected increases by the same amount, but also declines because people recover. Recovered people are immune to the disease and, hence, stay recovered. The mathematical representation of the model is as follows:

$$S_{t+1} = S_t - \lambda_t I_t S_t \tag{3}$$

$$I_{t+1} = I_t + \lambda_t I_t S_t - \gamma I_t \tag{4}$$

$$R_{t+1} = R_t + \gamma I_t, \tag{5}$$

where $N = S_t + I_t + R_t$ is the overall population and λ_t is the transmission rate of the infection.

Hence, $p_t = \lambda_t I_t$ is the probability that a susceptible individual becomes infected at time t . In the classic model, the latter is assumed to be exogenous, constant, and homogeneous across groups. Even as agents become aware of the pandemic, it is assumed that they do not adjust their behavior. More recent versions of the SIR model incorporate the dependence of contact rates on the heterogeneous topology of the network of contacts and mobility of people across locations (see Colizza et al. (2007) and Pastor-Satorras and Vespignani (2001a,b) who include bosonic-type reaction-diffusion processes in SIR models). Other variants of the model incorporate the dependence of infection rates on the activity intensity of each node of the network (see Perra et al. (2012) for solving activity-driven SIR using mean-field theory and Moinet et al. (2018) who also introduce a parameter capturing an exogenous decay of the infection risk due to precautionary behavior).

In what follows, we modify the homogeneous SIR and the SIR-network model so as to take into account how agents adjust their social-activity intensity in response to health risk and how, in turn, their equilibrium choices affect the infection rates of others.

4. A Model of Decision-Theory Based Social Interactions for Pandemics

We develop SIR models, both homogeneous and with a network structure, in which the contact rate results from a decision problem on the extent of social interactions. Combining search and optimizing behavior in economics goes back to Diamond (1982).¹⁹ Other authors have introduced this feature in SIR models (see our literature review), but, to the best of our knowledge, none of them merge it with a network structure and analyze the impact of social preferences and community traits. In the context of our model, the infection shock spreads to the rest of the community conditionally on these traits and the network structure. We

¹⁹ See Petrongolo and Pissarides (2001) for a survey.

also derive the social planner’s problems for our model variants to highlight the role of the various externalities that emerge in our setup.

Furthermore, and in contrast to others, we distinguish the dynamic optimization problem of the susceptible, infected, and recovered individuals. Susceptible agents internalize the probability of getting infected, which corresponds to our fear index in the data. The dynamic optimization allows us to control also for time discounting or patience. Additionally, infected agents internalize the health risk for others only under altruistic preferences.²⁰ In the model, warm-glow preferences are used to capture aspects common to altruism or trust. The presence of different decision processes requires a modification of the matching function, as we detail below. Introducing endogenous social-activity intensity in a networked SIR model allows us to examine the effect of reciprocity among different interconnected groups.

We start with the homogeneous SIR model where all agents in the population are the same except that they are susceptible, infected, or recovered. We label the health status with the index $i \in \{S, I, R\}$. Transitions of susceptible individuals from state S to I depend on contacts with other people,²¹ and these in turn depend on the social-activity intensity of each individual in the population and on the general matching technology.²² The model is in discrete time, time goes up to the infinite horizon, and there is no aggregate or idiosyncratic uncertainty.

Each agent has a per-period utility function $U_t^i(x_{h,t}^i, x_{s,t}^i) = u^i(x_{h,t}^i, x_{s,t}^i) - c^i(x_{h,t}^i, x_{s,t}^i)$, where x_h^i denotes home activities and x_s^i denotes social activities. The function $u^i(x_h^i, x_s^i)$ has standard concavity properties and $u^i(x_h^i, 0) > 0$. The cost, $c^i(x_h^i, x_s^i)$, puts a constraint on the choice between home and social activities. At time t , a susceptible agent enjoys the per-period utility, expects to enter the infected state with probability p_t or to remain susceptible with probability $(1 - p_t)$, and chooses the amount of home and social activities by recognizing that

20 Such setup implicitly assumes that agents recognize their symptoms. As known, there are also asymptomatic agents. Extending our model so as to incorporate the latter would not affect the main channels that we discuss.

21 These can arise in, e.g., entertainment activities, other outside activities, or in the workplace.

22 Transitions for individuals in the infected group I to recovery R depend only on medical conditions related to the disease (mostly the health system) that are outside of an individual’s control.

social activity increases the risk of infection. The value function of a susceptible individual is as follows:

$$V_t^S = U(x_{h,t}^S, x_{s,t}^S) + \beta[p_t V_{t+1}^I + (1 - p_t)V_{t+1}^S], \quad (6)$$

where β is the time discount factor, corresponding to *Patience_g* in the data, while p_t is the probability of being infected. The latter depends on the amount of social activity of the susceptible and infected agents, on the average amount of social activity, $\bar{x}_{s,t}$, in the population, an exogenously given transmission rate η , capturing the transmissibility of the disease, as well as on the individual shares of each group $i = I, S, R$ in the population:

$$p_t = p_t(x_{s,t}^S, x_{s,t}^I, \bar{x}_{s,t}, \eta, S_t, I_t, R_t), \quad (7)$$

where

$$\bar{x}_{s,t} = \bar{x}_{s,t}^S \frac{S_t}{N_t} + \bar{x}_{s,t}^I \frac{I_t}{N_t} + \bar{x}_{s,t}^R \frac{R_t}{N_t} \quad (8)$$

and $\bar{x}_{s,t}^S$ is the average amount of social activity of the susceptible, $\bar{x}_{s,t}^I$ is the average amount of social activity of the infected and $\bar{x}_{s,t}^R$ is the average amount of social activity of the recovered.

To map the endogenous SIR model to the standard SIR model in equations (3) to (5), the following convention is used: $p_t = \lambda_t I_t$. The exact functional form of p_t is defined later on. For now, it suffices to assume that $\frac{\partial p_t(\cdot)}{\partial x_{s,t}^S} > 0$ and $p_t(0, \cdot) = 0$.

In the baseline model, infected individuals do not have any altruistic motive. This specification allows us to highlight clearly the role of altruism once introduced. Their Bellman equation, in absence of altruism, is:

$$V_t^I = U(x_{h,t}^I, x_{s,t}^I) + \beta[(1 - \gamma)V_{t+1}^I + \gamma V_{t+1}^R]. \quad (9)$$

Currently infected individuals will remain infected for an additional period with probability

$(1 - \gamma)$ or will recover with probability γ .²³ The value function of the recovered reads as follows:

$$V_t^R = U(x_{h,t}^R, x_{s,t}^R) + \beta V_{t+1}^R. \quad (10)$$

Susceptible individuals' first-order conditions with respect to $x_{h,t}$ and $x_{s,t}$ are as follows:

$$\frac{\partial U(x_{h,t}^S, x_{s,t}^S)}{\partial x_{h,t}^S} = 0 \quad (11)$$

$$\frac{\partial U(x_{h,t}^S, x_{s,t}^S)}{\partial x_{s,t}^S} + \beta \frac{\partial p_t(\cdot)}{\partial x_{s,t}^S} (V_{t+1}^I - V_{t+1}^S) = 0, \quad (12)$$

where it is reasonable to assume that $(V_{t+1}^I - V_{t+1}^S) < 0$.

Susceptible individuals internalize the drop in utility associated with the risk of infection caused by social activity, and choose a level of social activity which is lower than the one that they would choose in the absence of a pandemic. This parallels our empirical findings insofar as agents naturally reduce their mobility in response to increased fear of infection. Also, individuals reduce social interactions by more when the discount factor, i.e., β , is higher. This mirrors our empirical result that the degree of patience reduces mobility and, thus, renders lockdown policies less effective or less necessary.

The first-order conditions of the infected with respect to $x_{h,t}$ and $x_{s,t}$ read as follows:

$$\frac{\partial U(x_{h,t}^I, x_{s,t}^I)}{\partial x_{h,t}^I} = 0, \quad \frac{\partial U(x_{h,t}^I, x_{s,t}^I)}{\partial x_{s,t}^I} = 0. \quad (13)$$

Infected individuals choose a higher level of social activity than susceptible ones since they do not internalize the effect of their decision on the risk of infection for others. However, their level of social activity will in turn affect the overall infection rate. In Section 4.2, we will assume infected individuals to hold altruistic preferences. This will induce them to also internalize the effect of their actions on the infection rate of the susceptible.

²³ Infected individuals might have a lower utility than susceptible or recovered ones due to the disease. We capture this in our calibration of the simulated model by assigning an extra cost of being sick in the utility function.

Finally, the first-order conditions of the recovered individuals are as follows:

$$\frac{\partial U(x_{h,t}^R, x_{s,t}^R)}{\partial x_{h,t}^R} = 0, \quad \frac{\partial U(x_{h,t}^R, x_{s,t}^R)}{\partial x_{s,t}^R} = 0. \quad (14)$$

Recovered people, assuming that they are immune to another infection, choose the same level of social activity as they would in the absence of a pandemic.

4.1. The Matching Function, Geography, and the Infection Rate

Given the optimal choice of social-activity intensity, we can now derive the equilibrium infection probability in the decentralized equilibrium. This involves defining a matching function (similar to the ones in Diamond (1982) or Pissarides (2000)). The intensity of social interaction, x_s , corresponds to the number of times people leave their home or, differently speaking, the probability per unit of time of leaving the home. In each one of these outside activities, individuals come in contact with other individuals. How many contacts the susceptible individuals have with an infected individual depends on the average amount of social activities in the population. Given (8) and normalizing the population size to one, the latter is given by $\bar{x}_{s,t} = S_t \bar{x}_{s,t}^S + I_t \bar{x}_{s,t}^I + R_t \bar{x}_{s,t}^R$. More precisely, the aggregate number of contacts depends on a matching function, which itself depends on the aggregate average social activity, $\bar{x}_{s,t}$, and can be specified as follows: $m(\bar{x}_{s,t}^S, \bar{x}_{s,t}^I, \bar{x}_{s,t}^R) = (\bar{x}_{s,t})^\alpha$.

The parameter α captures the matching function's returns to scale, ranging from constant to increasing. As such, this parameter captures, e.g., the geographic aspects of the location in which the disease spreads. Cities with denser logistical structures induce a larger number of overall contacts per outside activity. These could be, for example, cities with highly ramified underground transportation systems. In such locations, citizens tend to use public transport more frequently, and their likelihood of encountering infected individuals is subsequently larger. Mapping the geographical diversity is important also since our empirical analysis suggests that the uptake of public transit reacts more to fear (see Table 3).

Given the aggregate number of contacts, the average number of contacts per outside activity is given by $\frac{m(\bar{x}_{s,t})}{\bar{x}_{s,t}}$. Under the matching-function specification adopted above, this

can be written as $(\bar{x}_{s,t})^{(\alpha-1)}$. The probability of becoming infected depends also on the joint probability that susceptible and infected individuals both go out, which is given by $x_{s,t}^S x_{s,t}^I$, on the infection transmission rate, η , and on the number of infected individuals in the population, I_t . Therefore, we can denote the infection probability in the decentralized equilibrium as:

$$p_t(\cdot) = \eta x_{s,t}^S x_{s,t}^I \frac{m(\bar{x}_{s,t}^S, \bar{x}_{s,t}^I, \bar{x}_{s,t}^R)}{\bar{x}_{s,t}} I_t = \eta x_{s,t}^S x_{s,t}^I (\bar{x}_{s,t})^{\alpha-1} I_t. \quad (15)$$

Note that atomistic agents take the fraction of outside activities of other agents as given. If $\alpha = 0$, the probability $p_t = \eta x_{s,t}^S x_{s,t}^I \bar{x}_{s,t}^{-1} I_t$ is homogeneous of degree one, implying constant returns to scale, while if $\alpha = 1$, the probability becomes a quadratic function (see Diamond (1982)), as a consequence of which it exhibits increasing returns to scale.

The baseline SIR model in the decentralized equilibrium can now be re-written as follows:

$$S_{t+1} = S_t - p_t S_t \quad (16)$$

$$I_{t+1} = I_t + p_t S_t - \gamma I_t \quad (17)$$

$$R_{t+1} = R_t + \gamma I_t, \quad (18)$$

where $S_t + I_t + R_t \equiv 1$.

Definition 1. A decentralized equilibrium is a sequence of state variables, S_t, I_t, R_t , a set of value functions, V_t^S, V_t^I, V_t^R , and a sequence of home consumption, probabilities, and social activities, $p_t, x_{h,t}^S, x_{h,t}^I, x_{h,t}^R, x_{s,t}^S, x_{s,t}^I, x_{s,t}^R$, such that:

1. S_t, I_t, R_t solve (16) to (18), with the probability of infection given by (15)
2. V_t^S, V_t^I, V_t^R solve (6), (9), and (10)
3. The sequence $p_t, x_{h,t}^S, x_{h,t}^I, x_{h,t}^R, x_{s,t}^S, x_{s,t}^I, x_{s,t}^R$ solves (11), (12), (13), and (14).

Note that underlying the decentralized economy is a Nash symmetric equilibrium in the choice of social intensity.²⁴

²⁴ Ultimately, this can be micro-founded with global-games and higher-thinking considerations.

4.2. Altruism of Infected Individuals

Our empirical results have highlighted that the degrees of altruism and trust matter. Those two traits include variants of more or less selfish thinking. Altruism might arise from the pure pleasure of doing good, while trust embeds some degree of future reciprocation and is more generalized towards strangers.²⁵ In the model, we aim to mimic these traits. Specifically, warm-glow preferences are used to capture common features of altruism and trust, namely the utility enhancement of doing good. It is reasonable to conjecture that infected individuals hold some altruistic preferences. These attitudes may include both warm-glow preferences towards relatives and friends (see Becker (1974))²⁶ or general unconditional altruism and social preferences.²⁷ For this reason, we now extend the per-period utility so as to incorporate altruistic preferences by defining it as follows:

$$U(x_{h,t}^I, x_{s,t}^I) = u(x_{h,t}^I, x_{s,t}^I) - c(x_{h,t}^I, x_{s,t}^I) + \delta V_t^S. \quad (19)$$

While infected individuals do not internalize the effect of their social activities on the infection rate fully, as they are already immune in the near future, they do hold an altruistic motive towards the susceptible, which is captured by a weight $\delta \in (0, 1)$. The first-order condition with respect to the social activity changes to:

$$\frac{\partial U(x_{h,t}^I, x_{s,t}^I)}{\partial x_{s,t}^I} + \delta \beta \frac{\partial p_t(\cdot)}{\partial x_{s,t}^I} (V_{t+1}^I - V_{t+1}^S) = 0. \quad (20)$$

Now the optimal level of social activity chosen by infected individuals is lower than the one obtained under (13) since they partly internalize the risk of infecting susceptible individuals, who then turn into infected ones next period. Time discounting is also relevant in this context: more patient individuals tend to internalize the impact of their social activity on the infection probability by more.

²⁵ See Berg et al. (1995), Bohnet and Frey (1999), Andreoni (1989), or Andreoni (1993).

²⁶ Warm-glow preferences have a long-standing tradition in economics. Besides Becker (1974)'s original work, see Andreoni (1989) as well as Andreoni (1993).

²⁷ See, for instance, Bolton and Ockenfels (2000) or Andreoni and Miller (2002).

4.3. Extension to an SIR-Network Model

Within communities there are different groups that have different exposure or contact rates to each one of the other groups. Homophily in networks describes the likelihood that two nodes (groups) are linked only to a small degree to each other or “the tendency of various types of individuals to associate with others who are similar to themselves” (see Currarini et al. (2009)).²⁸ We use homophily to map the role of reciprocity in our data. Higher homophily is associated with less negative reciprocity. The SIR model is then extended so as to include different groups of the population that experience different contact rates due to differential degrees of homophily. These groups could correspond to, e.g., the age structure, different strengths in ties, or closer face-to-face interactions in the workplace. The underlying idea is that contact rates tend to be higher among peer groups.

Consider a population with different groups $j = 1, \dots, J$. The number of people in each group is N_j . Groups have different probabilities of encounters with the other groups. The contact intensity between group j and any group k is $\xi_{j,k}$. The latter captures differential degrees of homophily within groups. Younger individuals tend to meet other young ones, i.e., their peers, more often. Also, workers in face-to-face occupations enter more often in contacts with workers performing similar tasks. This implies that the infection outbreak may be concentrated among members of the same group. Whether the outbreak then spreads to the rest of the network, and how fast it does so, depends on the relative degree of attachment of the initially infected group to the other groups. At last, in our simulations we realistically allow for differential recovery rates in different age groups, with older agents being more fragile than younger ones.

Each susceptible individual of group j experiences a certain number of contacts per outing with infected individuals of his own group, but also of the other groups. Reflecting our discussion in Section 4.1, the number of contacts experienced by group j depends on the

²⁸ See also Fehr and Schmidt (1999) or Fehr and Gächter (2000).

average level of social activity in each group k weighted by the contact intensity across groups, and is equal to:

$$m^j(\hat{x}_{s,t}^j) = m^j \left(\sum_k \xi_{j,k} (\bar{x}_{s,t}^{S,k} S_t^k + \bar{x}_{s,t}^{I,k} I_t^k + \bar{x}_{s,t}^{R,k} R_t^k) \right). \quad (21)$$

As before, the matching function can be specified as $m^j(\hat{x}_{s,t}^j) = \left(\sum_k \xi_{j,k} (\bar{x}_{s,t}^{S,k} S_t^k + \bar{x}_{s,t}^{I,k} I_t^k + \bar{x}_{s,t}^{R,k} R_t^k) \right)^\alpha$.

The probability of infection of a susceptible person in group j is modified as follows:

$$p_t^j(\cdot) = x_{s,t}^{S,j} \left[\sum_k \eta \xi_{j,k} x_{s,t}^{I,k} \frac{m^j(\hat{x}_{s,t}^j)}{\hat{x}_{s,t}^j} I_t^k \right], \quad (22)$$

where $k = 1, \dots, J$ and $\xi_{j,j} = 1$. The underlying rationale is equivalent to the one described in the single-group case, except that now the probability of meeting an infected person from any other group k is weighted by the likelihood of the contacts across groups, $\xi_{j,k}$.

The SIR model for each group j then reads as follows:

$$S_{t+1}^j = S_t^j - p_t^j(\cdot) S_t^j \quad (23)$$

$$I_{t+1}^j = I_t^j + p_t^j(\cdot) S_t^j - \gamma I_t^j \quad (24)$$

$$R_{t+1}^j = R_t^j + \gamma I_t^j, \quad (25)$$

where $\sum_j (S_t^j + I_t^j + R_t^j) \equiv 1$.

As before, atomistic individuals take the average social activity and the average social encounters as given. The first-order condition for social activity of susceptible individuals belonging to group j now reads as follows:

$$\frac{\partial U(x_{h,t}^{S,j}, x_{s,t}^{S,j})}{\partial x_{s,t}^{S,j}} + \beta \left[\sum_k \eta \xi_{j,k} x_{s,t}^{I,k} \frac{m^j(\hat{x}_{s,t}^j)}{\hat{x}_{s,t}^j} I_t^k \right] (V_{t+1}^{I,j} - V_{t+1}^{S,j}) = 0. \quad (26)$$

Each susceptible agent takes the average level of social activity by the others as given. It becomes clear that the differential impact of her social activity on the various groups affects her optimal choice.

We can now derive the first-order conditions of the infected. For this purpose, we assume

altruistic preferences, which means that infected agents internalize, at least partly, with the weight δ , the impact of their choices on the susceptible agents of all other groups. The first-order condition with respect to social activity is:

$$\frac{\partial U(x_{h,t}^{I,j}, x_{s,t}^{I,j})}{\partial x_{s,t}^{I,j}} + \delta\beta \sum_k x_{s,t}^{S,k} \eta \xi_{k,j} \frac{m^k(\hat{x}_{s,t}^k)}{\hat{x}_{s,t}^k} I_t^j (V_{t+1}^{I,k} - V_{t+1}^{S,k}) = 0. \quad (27)$$

The first-order conditions for the recovered individuals are the same as in (14), but separately for each group j .

Definition 2. *A decentralized equilibrium for the SIR-network model is a sequence of state variables, S_t^j, I_t^j, R_t^j , a set of value functions, $V_t^{S,j}, V_t^{I,j}, V_t^{R,j}$, and a sequence of home consumption, probabilities, and social activities, $p_t^j, x_{h,t}^{S,j}, x_{h,t}^{I,j}, x_{h,t}^{R,j}, x_{s,t}^{S,j}, x_{s,t}^{I,j}, x_{s,t}^{R,j}$, such that:*

1. S_t^j, I_t^j, R_t^j solve (23) to (25) for each group j , with the probability of infection given by (22) for each group j
2. $V_t^{S,j}, V_t^{I,j}, V_t^{R,j}$ solve (6), (9), and (10), now defined separately for each group j
3. The sequence $p_t^j, x_{h,t}^{S,j}, x_{h,t}^{I,j}, x_{h,t}^{R,j}, x_{s,t}^{S,j}, x_{s,t}^{I,j}, x_{s,t}^{R,j}$ solves (26), (27), (11), the second part of (13), and (14) for each group j .

4.4. Social Planner

As noted before, when each person chooses her optimal social activity, she does not consider its impact on the average level of social activity nor on the future course of the number of infected individuals. A social planner takes both into account. The planner's problem is derived for both the homogeneous SIR and the networked SIR.

The planner is aware of how the average social activity is affected by the density of the matching function (corresponding to, e.g., the geography of the city) and of the future course of infected individuals.²⁹ The planner knows that in a Nash equilibrium each agent chooses the same amount of social activity, so individual and average social interactions are now the

²⁹ The planner is aware of the SIR structure, namely the technological constraints, and can decide on policies taking into account the transitions across the different health states.

same, hence $x_{s,t}^S = \bar{x}_{s,t}^S$ and $x_{s,t}^I = \bar{x}_{s,t}^I$. This implies that the equilibrium infection rate is given by:

$$p_t^P(\cdot) = \eta x_{s,t}^S x_{s,t}^I (S_t x_{s,t}^S + I_t x_{s,t}^I + R_t x_{s,t}^R)^{(\alpha-1)} I_t. \quad (28)$$

Definition 3: Social Planner in the Homogeneous SIR Model. The social planner chooses the paths of home and social, i.e., outside, activities for each agent by maximizing the weighted sum of the utilities of all agents. The planner is aware of the dependence of the value function of susceptible individuals on the total number of infected and susceptible individuals. Hence, we distinguish between the value function in the decentralized equilibrium and in the planner economy, with the latter denoted as \hat{V}^i where $i = I, S, R$. The planner chooses the sequence $[S_{t+1}, I_{t+1}, R_{t+1}, x_{h,t}^S, x_{h,t}^I, x_{h,t}^R, x_{s,t}^S, x_{s,t}^I, x_{s,t}^R]_{t=0}^\infty$ at any initial period t to maximize:

$$\hat{V}_t^N = S_t \hat{V}_t^S(S_t, I_t) + I_t \hat{V}_t^I + R_t \hat{V}_t^R \quad (29)$$

with

$$\hat{V}_t^S(S_t, I_t) = U(x_{h,t}^S, x_{s,t}^S) + \beta [p_t^P(\cdot) \hat{V}_{t+1}^I + (1 - p_t^P(\cdot)) \hat{V}_{t+1}^S] \quad (30)$$

$$\hat{V}_t^I = U(x_{h,t}^I, x_{s,t}^I) + \delta \hat{V}_t^S(S_t, I_t) + \beta [(1 - \gamma) \hat{V}_{t+1}^I + \gamma \hat{V}_{t+1}^S] \quad (31)$$

$$\hat{V}_t^R = U(x_{h,t}^R, x_{s,t}^R) + \beta \hat{V}_{t+1}^R \quad (32)$$

subject to

$$S_{t+1} = S_t - p_t^P(\cdot) S_t \quad (33)$$

$$I_{t+1} = I_t + p_t^P(\cdot) S_t - \gamma I_t \quad (34)$$

$$R_{t+1} = R_t + \gamma I_t, \quad (35)$$

where $S_t + I_t + R_t \equiv 1$.

Proposition 1. *The planner reduces social interactions on top and above the decentralized equilibrium. She does so due to a static and a dynamic externality.*

Proof. The first-order conditions for home activities of susceptible and infected individuals

and for all activities of the recovered remain the same as in the decentralized equilibrium. The choices of the social activities of susceptible and infected agents are derived in Appendix B. The size of the aggregate inefficiency is obtained from the difference between the first-order conditions for social activities of susceptible and infected individuals in the decentralized equilibrium, (12) and (20), and the corresponding ones for the social planner's solution, (55) and (56):

$$\chi_t^S = \beta \left[\frac{\partial p_t^P(\cdot)}{\partial x_{s,t}^S} - \frac{p_t}{x_{s,t}^S} \right] [\hat{V}_{t+1}^I - \hat{V}_{t+1}^S] + \beta(1 - p_t^P(\cdot)) \left[\frac{\partial \hat{V}_{t+1}^S}{\partial S_{t+1}} \frac{\partial S_{t+1}}{\partial x_{s,t}^S} + \frac{\partial \hat{V}_{t+1}^S}{\partial I_{t+1}} \frac{\partial I_{t+1}}{\partial x_{s,t}^S} \right] = 0 \quad (36)$$

$$\chi_t^I = \delta \left\{ \beta \left[\frac{\partial p_t^P(\cdot)}{\partial x_{s,t}^I} - \frac{p_t}{x_{s,t}^I} \right] [\hat{V}_{t+1}^I - \hat{V}_{t+1}^S] + \beta(1 - p_t^P(\cdot)) \left[\frac{\partial \hat{V}_{t+1}^S}{\partial S_{t+1}} \frac{\partial S_{t+1}}{\partial x_{s,t}^I} + \frac{\partial \hat{V}_{t+1}^S}{\partial I_{t+1}} \frac{\partial I_{t+1}}{\partial x_{s,t}^I} \right] \right\} = 0, \quad (37)$$

where $p_t^P(\cdot)$ is given by (28).

These differences can be decomposed into two parts corresponding to a static and a dynamic inefficiency.³⁰ First, atomistic agents do not internalize the impact of their decisions on the average level of social activity, while the planner does. In other words, when choosing their social activity, the atomistic agents take into account the infection rate given by (15), while the social planner takes into account the infection rate given by (28). Hence, the static inefficiency is given by:

$$\Phi_t^S = \beta \left[\frac{\partial p_t^P(\cdot)}{\partial x_{s,t}^S} - \frac{p_t(\cdot)}{x_{s,t}^S} \right] [V_{t+1}^{\hat{I}} - V_{t+1}^{\hat{S}}] \quad (38)$$

$$\Phi_t^I = \delta \beta \left[\frac{\partial p_t^P(\cdot)}{\partial x_{s,t}^I} - \frac{p_t(\cdot)}{x_{s,t}^I} \right] [V_{t+1}^{\hat{I}} - V_{t+1}^{\hat{S}}], \quad (39)$$

where $\frac{p_t(\cdot)}{x_{s,t}^i} = \frac{\partial p_t(\cdot)}{\partial x_{s,t}^i}$, for $i = S, I$. The static inefficiency is affected by the matching function's returns to scale. In places with more dense interactions, the spread of the disease is faster and the size of the inefficiency is larger. This implies that the social planner will adopt

³⁰ These inefficiencies are also considered in Garibaldi et al. (2020) in a different model setup.

stringency or non-pharmaceutical interventions (henceforth NPIs) on top and above the restraints applied by both the susceptible and the infected.

The second components that distinguish (55) and (56) from (12) and (20) are:

$$\Psi_t^S = \beta(1 - p_t^P(\cdot)) \left[\frac{\partial \hat{V}_{t+1}^S}{\partial S_{t+1}} \frac{\partial S_{t+1}}{\partial x_{s,t}^S} + \frac{\partial \hat{V}_{t+1}^S}{\partial I_{t+1}} \frac{\partial I_{t+1}}{\partial x_{s,t}^S} \right] \quad (40)$$

$$\Psi_t^I = \delta\beta(1 - p_t^P(\cdot)) \left[\frac{\partial \hat{V}_{t+1}^S}{\partial S_{t+1}} \frac{\partial S_{t+1}}{\partial x_{s,t}^I} + \frac{\partial \hat{V}_{t+1}^S}{\partial I_{t+1}} \frac{\partial I_{t+1}}{\partial x_{s,t}^I} \right]. \quad (41)$$

These terms identify a dynamic inefficiency, which arises since the planner acts under commitment. The planner recognizes that next period's number of infected and susceptible individuals is going to have an effect on the value function of the susceptible individuals through future infection rates.

Definition 4: Social Planner in the SIR-Network Model. In the SIR-network model, the social planner maximizes the sum of future discounted utilities of all groups in the population, taking as given that the infection rates depend on the Nash equilibrium of social interactions. This implies that the infection rates in the networked SIR equilibrium are given by:

$$p_t^{Pj}(\cdot) = x_{s,t}^{S,j} \left[\sum_k \eta \xi_{j,k} x_{s,t}^{I,k} \frac{m^j \left(\sum_k \xi_{j,k} (x_{s,t}^{S,k} S_t^k + x_{s,t}^{I,k} I_t^k + x_{s,t}^{R,k} R_t^k) \right)}{\sum_k \xi_{j,k} (x_{s,t}^{S,k} S_t^k + x_{s,t}^{I,k} I_t^k + x_{s,t}^{R,k} R_t^k)} I_t^k \right]. \quad (42)$$

The planner now chooses the sequence $[S_{t+1}^j, I_{t+1}^j, R_{t+1}^j, x_{h,t}^{S,j}, x_{h,t}^{I,j}, x_{h,t}^{R,j}, x_{s,t}^{S,j}, x_{s,t}^{I,j}, x_{s,t}^{R,j}]_{t=0}^\infty$ at any initial period t and for all j to maximize:

$$\hat{V}_t^N = \sum_j [S_t^j \hat{V}_t^{S,j} + I_t^j \hat{V}_t^{I,j} + R_t^j \hat{V}_t^{R,j}] \quad (43)$$

with

$$\hat{V}_t^{S,j}(S_t^j, I_t^j) = U(x_{h,t}^{S,j}, x_{s,t}^{S,j}) + \beta[p_t^{Pj} \hat{V}_{t+1}^{I,j} + (1 - p_t^{Pj}) \hat{V}_{t+1}^{S,j}] \quad (44)$$

$$\hat{V}_t^{I,j} = U(x_{h,t}^{I,j}, x_{s,t}^{I,j}) + \delta \sum_j \hat{V}_t^{S,j}(S_t^j, I_t^j) + \beta[(1 - \gamma)\hat{V}_{t+1}^{I,j} + \gamma\hat{V}_{t+1}^{S,j}] \quad (45)$$

$$\hat{V}_t^{R,j} = U(x_{h,t}^{R,j}, x_{s,t}^{R,j}) + \beta[\hat{V}_{t+1}^{R,j}] \quad (46)$$

subject to

$$S_{t+1}^j = S_t^j - p_t^{Pj}(\cdot)S_t^j \quad (47)$$

$$I_{t+1}^j = I_t^j + p_t^{Pj}(\cdot)S_t^j - \gamma I_t^j \quad (48)$$

$$R_{t+1}^j = R_t^j + \gamma I_t^j, \quad (49)$$

where $\sum_j (S_t^j + I_t^j + R_t^j) \equiv 1$. The full set of first-order conditions can be found in Appendix C.

Proposition 2. *The inefficiencies in the SIR-network model are larger than in the homogeneous SIR model, and also take into account the reciprocal relations.*

Proof. The first-order conditions of the planner problem can be found in Appendix C. Comparing those, i.e., (57) and (58), with the corresponding ones from the decentralized equilibrium of the SIR-network model, we obtain the following aggregate inefficiencies for each group j :

$$\Omega_t^{S,j} = \beta \left[\frac{\partial p_t^{Pj}(\cdot)}{\partial x_{s,t}^{S,j}} - \frac{\partial p_t^j}{\partial x_{s,t}^{S,j}} \right] [\hat{V}_{t+1}^{I,j} - \hat{V}_{t+1}^{S,j}] + \beta(1 - p_t^{Pj}(\cdot)) \sum_k \left[\frac{\partial \hat{V}_{t+1}^{S,j}}{\partial S_{t+1}^k} \frac{\partial S_{t+1}^k}{\partial x_{s,t}^{S,j}} + \frac{\partial \hat{V}_{t+1}^{S,j}}{\partial I_{t+1}^k} \frac{\partial I_{t+1}^k}{\partial x_{s,t}^{S,j}} \right] = 0 \quad (50)$$

$$\Omega_t^{I,j} = \delta\beta \sum_k \left\{ \left[\frac{\partial p_t^{Pk}(\cdot)}{\partial x_{s,t}^{I,j}} - \frac{\partial p_t^k}{\partial x_{s,t}^{I,j}} \right] [\hat{V}_{t+1}^{I,k} - \hat{V}_{t+1}^{S,k}] + (1 - p_t^{Pk}(\cdot)) \sum_n \left[\frac{\partial \hat{V}_{t+1}^{S,k}}{\partial S_{t+1}^n} \frac{\partial S_{t+1}^n}{\partial x_{s,t}^{I,j}} + \frac{\partial \hat{V}_{t+1}^{S,k}}{\partial I_{t+1}^n} \frac{\partial I_{t+1}^n}{\partial x_{s,t}^{I,j}} \right] \right\} = 0. \quad (51)$$

For the SIR-network model, the inefficiencies contain additional components. First of all, the static inefficiency is summed across all groups j . Second, the dynamic inefficiency is weighted by a probability that takes into account the summation of the infection rates across groups. These additional terms capture a reciprocity externality. The planner is aware that the social activity has a differential impact across age groups, which is reflected in the size of the externality.

Having characterized the inefficiencies, we turn to discussing actual implementation policies in the homogeneous SIR and the SIR-network model, and their suitability to close the inefficiencies.

4.5. Implementability: Partial Lockdown in the Homogeneous SIR Model and Targeted Lockdown in the SIR-Network Model

In this section, we examine which lockdown policies are efficient. In particular, we consider partial and targeted lockdown policies.

Partial Lockdown in SIR. A partial lockdown can be examined also in the simple homogeneous SIR model. θ is defined as the fraction of social activity that is restricted. The planner can enforce two different lockdown policies, θ^S and θ^I , only if there is the possibility to identify infected individuals. Let us first assume they cannot be identified, so the social activity of all agents will be restricted.³¹ Furthermore, there is only a unique θ . Then, a partial lockdown policy affects the infection probability in the decentralized economy as follows:

$$p_t(\theta, \cdot) = \eta(1 - \theta)x_{s,t}^S(1 - \theta)x_{s,t}^I \frac{m((1 - \theta)\bar{x}_{s,t})}{(1 - \theta)\bar{x}_{s,t}} I_t. \quad (52)$$

Lemma 1. *The partial lockdown policy is efficient only in the presence of the means to identify infected individuals, such as universal testing.*

Proof. The partial lockdown policy would be efficient if it set the aggregate inefficiencies equal to zero, that is:

$$\beta \left[\frac{\partial p_t^P(\cdot)}{\partial x_{s,t}^S} - \frac{p_t}{x_{s,t}^S} \right] [\hat{V}_{t+1}^I - \hat{V}_{t+1}^S] + \beta(1 - p_t^P(\cdot)) \left[\frac{\partial \hat{V}_{t+1}^S}{\partial S_{t+1}} \frac{\partial S_{t+1}}{\partial x_{s,t}^S} + \frac{\partial \hat{V}_{t+1}^S}{\partial I_{t+1}} \frac{\partial I_{t+1}}{\partial x_{s,t}^S} \right] = 0 \quad (53)$$

³¹ Some individuals might not have any symptoms and are not tested.

$$\delta\beta \left\{ \left[\frac{\partial p_t^P(\cdot)}{\partial x_{s,t}^I} - \frac{p_t}{x_{s,t}^I} \right] [\hat{V}_{t+1}^I - \hat{V}_{t+1}^S] + (1 - p_t^P(\cdot)) \left[\frac{\partial \hat{V}_{t+1}^S}{\partial S_{t+1}} \frac{\partial S_{t+1}}{\partial x_{s,t}^I} + \frac{\partial \hat{V}_{t+1}^S}{\partial I_{t+1}} \frac{\partial I_{t+1}}{\partial x_{s,t}^I} \right] \right\} = 0. \quad (54)$$

Equations (53) and (54) include both the static and the dynamic inefficiency. If the planner is endowed with a single instrument, i.e., a single lockdown policy applied equally to both susceptible and infected individuals, she cannot close these two inefficiencies at once. Only in the presence of a second instrument, specifically a measure to identify infected individuals, she can target policies toward agents in these two states and set the inefficiencies to zero.

Targeted Lockdown Policies in the SIR-Network Model. In the SIR-network model, the planner could consider targeted policies, i.e., different degrees of stringency measures targeted at different groups.

Lemma 2. *Implementable targeted lockdown policies require differentiated fractions θ_j^S and θ_j^I for susceptible and infected individuals of each group. This can be achieved only with the additional instrument of testing.*

Proof. Targeted lockdown policies would be efficient if they could set to zero the aggregate inefficiencies stemming from (50) and (51). This would imply different θ_j^S and θ_j^I that can close the $2j$ inefficiencies. This can be achieved only by means of identifying and isolating infected from susceptible individuals.

5. Simulations

In this section, we simulate different variants of our model, both in the decentralized equilibrium and under the social planner's equilibrium. The primary goal is to ascertain the impact of social-activity choices on the dynamics of infections by comparing our baseline optimizing SIR model to the traditional variant with exogenous contact rates. Furthermore, by comparing the simulations of the homogeneous SIR model with and without altruism, we

assess the latter’s importance. Finally, simulations of the SIR-network model highlight the role of reciprocity.

Overall, all model variants in which agents adjust their social activity in response to risk, altruism, and homophily exhibit a flattened infection curve compared to the traditional SIR model. This enhances the salience of our model implications. Policymakers designing mitigation policies shall be aware of the agents’ responses to risk, also conditional upon their social, cultural, and community traits.

5.1. Comparison Homogeneous SIR Model with Optimizing Individuals and Standard SIR Model

The model is solved numerically through a classical Newton-Raphson algorithm that computes the transition from one steady state to the next, with the latter induced by an infection shock leading to changes in the number of infected individuals in the population. The model calibration is as follows. The instantaneous utility of the susceptible and infected is a function of their social activities $x_{s,t}^S$ and $x_{s,t}^I$, respectively.³² The functional forms read as follows: $U(x_{s,t}^S) = x_{s,t}^S - \frac{(x_{s,t}^S)^2}{2c_S}$ and $U(x_{s,t}^I) = x_{s,t}^I - \frac{(x_{s,t}^I)^2}{2c_I} - C_I$, where C_I is the cost of being sick, and we set $c_S = 1$ and $c_I = 0.5$. In general, C_I might depend on the congestion of the health system, which in turn depends on the number of infected individuals. We abstract from this dependence, but note that its inclusion would actually strengthen our conclusions: infected individuals aware of the health-system congestion would reduce their social activity even more.

The cost of being sick is set equal to 10. This is a relatively high value, which reflects fear of severe long-term health complications or even death. Recall that for simplicity, in our analytical derivations we have assumed a death rate of zero, so it is reasonable to include its impact among the costs of the infection. Following Newman (2018), we set the recovery rate γ to 0.4. Furthermore, β is set to 0.95 and δ to 0.5. Following Garibaldi et al. (2020), we

³² We assume that in steady state the utility function of recovered and susceptible individuals are the same. Recovered individuals do not modify their social activity since they become immune. This is realistic at least for a certain length of time. Furthermore, in the simulations we do not analyze the home activities since they do not matter for our results.

set $\eta = 2.2$, which combines a constant term from the matching function and the exogenous transmission rate of COVID-19.

Figure 3 below compares the dynamics of the numbers of infected, susceptible, and recovered individuals both in our homogeneous SIR model with endogenous social activity and in the traditional SIR model with exogenous contact rates. For the sake of comparison, in the latter the social activity is set to a constant value equal to the average steady-state social activity, i.e., 0.75. The other parameters are the same across the two models. Furthermore, Figure 4 shows the dynamics of the social activity chosen by infected individuals, and compares the models with and without altruism.

First and foremost, Figure 3 shows that the peak of the infection curve (middle panel) is significantly flattened in the model with endogenous social activity. The number of susceptible individuals remains higher in the optimizing SIR model. As the disease takes its course, the number of infected individuals increases more sluggishly over time. An exact quantification of this effect could be useful for the planning of health care units. Second, Figure 4 shows that the social interaction of infected individuals (left panel) is unchanged over time in the absence of altruism, while it decreases significantly in the presence of altruism. Interestingly, in the presence of altruism, susceptible individuals decrease their social contacts by less, since part of the burden is carried by the infected individuals.

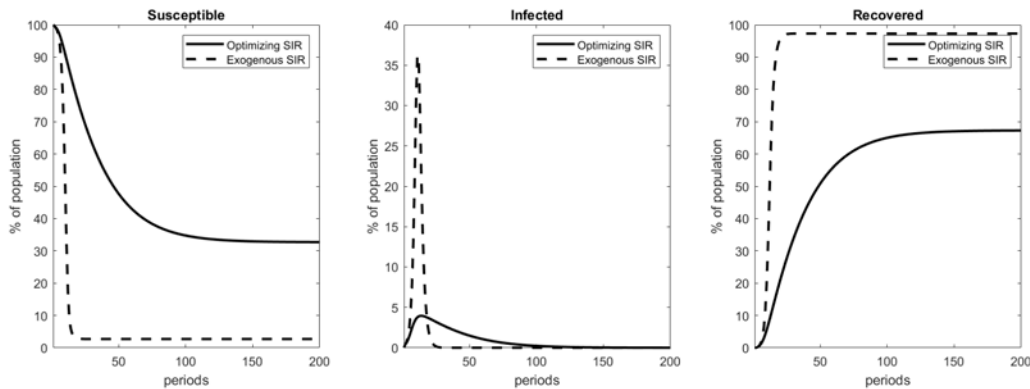


Figure 3

Comparison of the Homogeneous SIR Model with Endogenous Social Activity and the Traditional SIR Model with Constant Exogenous Contact Rates

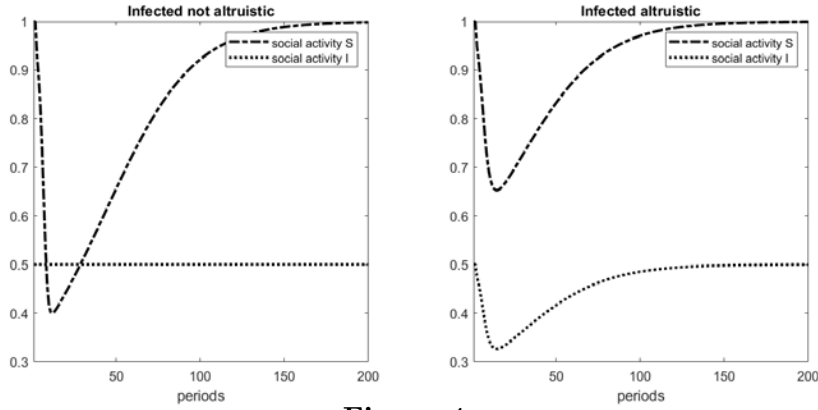


Figure 4

Comparison of Social Activity of Infected and Susceptible Individuals in the Homogeneous SIR Model with (right panel) and without Altruism (left panel)

5.1.1. Comparison SIR-Network Model with Endogenous Social Activity and Standard SIR-Network Model

In the SIR-network model, three age groups are included.³³ Following Acemoglu et al. (2020), the three groups are the young (20 – 49 years), middle-aged (50 – 64 years), and old (65+ years). The respective population shares are set to $N_y = 53\%$, $N_m = 26\%$, and $N_o = 21\%$. The network adjacency or homophily matrix is calibrated so that all groups have a contact rate, $\xi_{j,k}$, equal to 1 with their peers and equal to 0.7 (or later on 0.4) with the other groups. The matrix is symmetric. This calibration is similar to that in Acemoglu et al. (2020), which facilitates the comparison of our SIR-network model with endogenous social activity and other SIR-network models with exogenous contact rates and similar age structures. Realistically, different age groups have different recovery rates. For the middle-aged group, we set $\gamma_m = 0.4$, a number that is standard in the literature; for the younger group, a slightly faster recovery $\gamma_y = 0.45$ is chosen, and for the older group, we set $\gamma_o = 0.35$. All other parameters are kept as in the benchmark homogeneous SIR model.

Figure 5 compares the dynamics of infected, susceptible, and recovered individuals in our SIR-network model (thicker lines) with those in the exogenous SIR-network model (thinner lines).³⁴ The latter case is obtained by setting the social activity of each group equal to their

³³ An extension to more groups is feasible, but would not change the main implications.

³⁴ The initial infection shock is set to take place in the young group, i.e., the group with the presumably higher social-activity intensity.

respective steady-state values. The comparison is again revealing. In our SIR-network model, the curves for the infected of all age groups are much flatter than those in the exogenous SIR-network model. Figure 6 displays the social activity of susceptible individuals of all three age groups for our model. While young, middle-aged, and old agents all reduce their social activities, the old group reduces it by more since its agents are more exposed to the severe health risk and the corresponding utility loss due to their lower recovery rate.

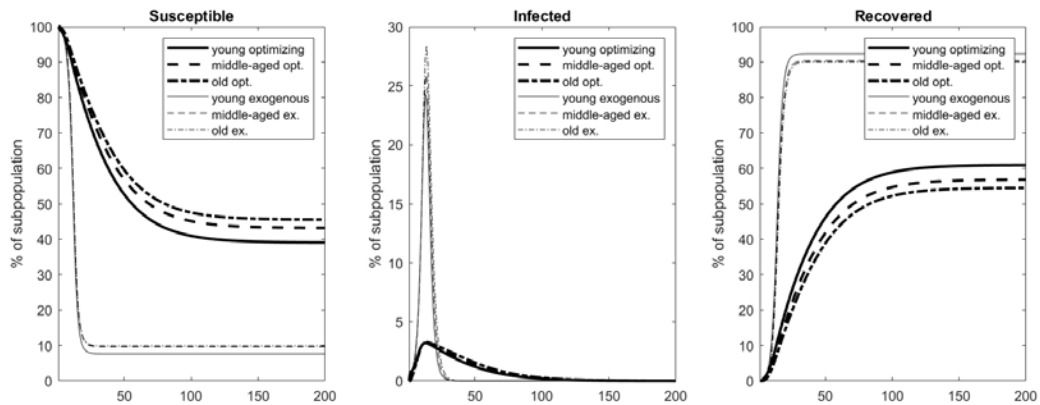


Figure 5

Comparison of SIR-Network Models with Endogenous Social Activity vs. Constant Exogenous Contact Rates

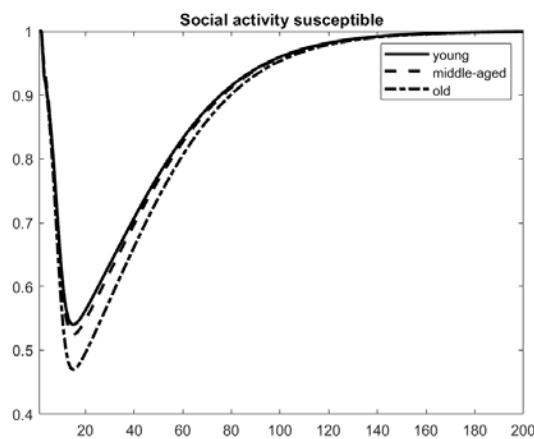


Figure 6

Dynamics of Social Interactions of Age Groups in the SIR-Network Model with Endogenous Social Activity

5.2. Optimal Lockdown Policy in the Homogeneous SIR and the SIR-Network Model: Social Planner’s Solution

We now quantify the optimal lockdown policy and its dependence on the preference and community structure, for both the homogeneous SIR and the networked SIR model. Figure 7 plots the optimal lockdown policy as captured by the fraction θ chosen by the planner (right panel) and the resulting social interactions of the susceptible individuals in our homogeneous SIR model with optimizing agents (the parameters are as before). Each panel compares the cases with (dashed line) and without altruism (solid line). Interestingly, and in accordance with our empirical results, the planner chooses a smaller fraction of locked-down activities when individuals are altruistic. Again, social interactions of susceptible individuals are higher in the altruistic case. This is because infected individuals adjust their interactions already by themselves in consideration of other people’s infection risk.

Figure 8 plots the optimal lockdown policy (right panel) and the resulting social interactions of the infected (left panel) for the planner’s solution in the SIR-network model. Here, lockdown policies are set differentially across age groups. While a full lockdown of a single group (sequestering) jointly with full freedom for the others would be unethical, joint burden sharing with differential protective NPIs across groups is desirable in light of the different recovery rates.³⁵ A practical implementation of this policy would include more extensive leave of absence for workers in older age groups or in groups with pre-existing health conditions.

Our results point to two main conclusions. First, stringency measures are stricter for the greatest risk spreaders, namely the age group in which the infection shock happened and which is in closer contact to other groups. Second, each panel compares the cases where individuals hold different degrees of homophily, setting $\xi = 0.7$ (lower homophily, black lines) and $\xi = 0.4$ (higher homophily, blue lines). Interestingly, stringency measures are generally stricter in the case of lower homophily. Lower homophily implies that an infection outbreak, occurring within one group, spreads faster to the other groups. Hence, in order to curb the epidemic, the planner optimally shall restrict social activity in the affected group by more.

³⁵ Recall that different recovery rates also implicitly capture different mortality rates.

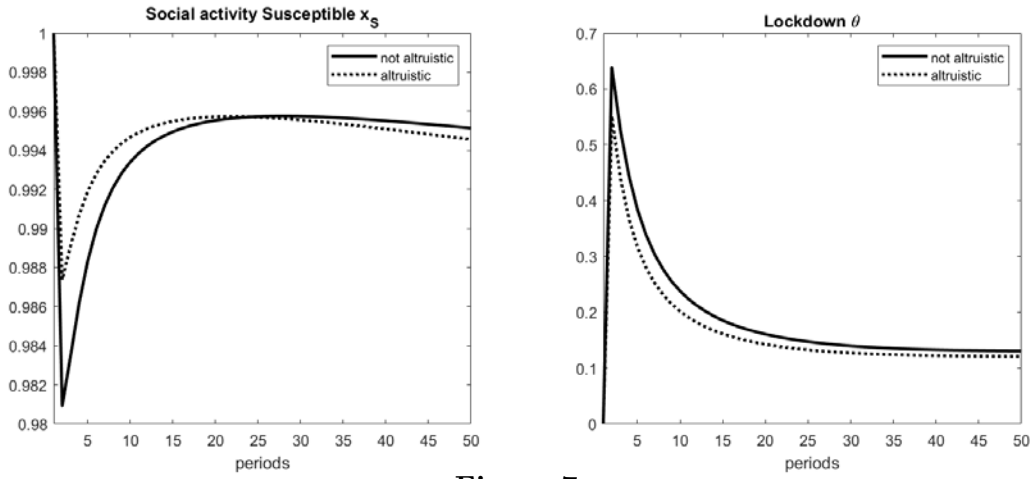


Figure 7
Social Activity of Susceptible Individuals and Optimal Lockdown Depending on Degree of Altruism of Infected Individuals

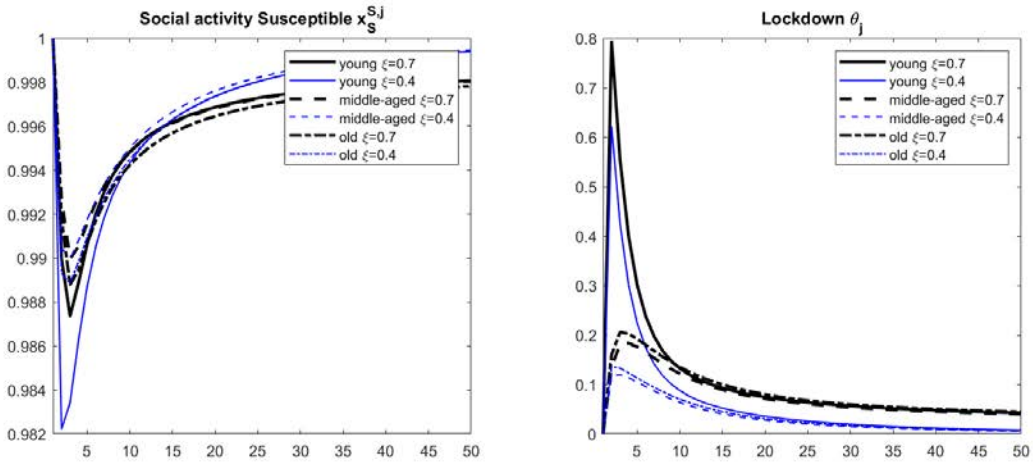


Figure 8
Social Activity of Susceptible Individuals and Optimal Differentiated Lockdown Policies for Different Degrees of Group Connections

6. Concluding Remarks

While envisaging a return to freedom of mobility and to past customs, though hopefully with fading fears, understanding the determinants of people’s behavior in the face of catastrophic events is important along at least two dimensions. First, it is difficult to accurately forecast the spread of a disease with models that do not account for human behavior. Second, as policymakers seek advice on exit strategies that could mitigate both the loss of lives and the economic consequences, understanding individuals’ behavior even as lockdowns or other

stringency measures are lifted is informative. Excessive precautionary behavior is likely to trigger demand spirals which might slow down the recovery process.

We use daily mobility data for 299 cities worldwide to show that preference traits, such as patience, altruism, and trust as well as community traits, such as reciprocity, matter for the behavioral response of individuals during a pandemic. We rationalize this behavior by proposing extensions of the homogeneous SIR and the SIR-network model that account for agents' optimizing behavior.

One of the initial approaches to contain the pandemic, suggested by experts, has been a "one size fits all" response, namely a full lockdown. We uncover important heterogeneities in individuals' behavior as well as in the efficacy of stringency measures with respect to regional differences in time and space. Our findings suggest that a balanced approach involving a joint interaction of stringency measures, in respect of human dignity, and responsible social preferences can help mitigate both the public health crisis and the economic costs. A social planner does wish to impose stringency measures, due to various externalities, but they depend on the social, cultural, and community traits. Stringency measures are stricter for agents with high social intensity and when groups exhibit less homophily, i.e., when the disease is less likely to be confined to one group, and can spread more easily within communities.

References

- Acemoglu, D., Chernozhukov, V., Werning, I., and Whinston, M. D. (2020). Optimal Targeted Lockdowns in a Multi-Group SIR Model. *NBER Working Paper No. 27102*.
- Alvarez, F., Argente, D., and Lippi, F. (2020). A Simple Planning Problem for COVID-19 Lockdown. *CEPR Discussion Paper No. 14658*.
- Ambrus, A., Mobius, M., and Szeidl, A. (2014). Consumption Risk-Sharing in Social Networks. *American Economic Review*, 104(1):149–182.
- Andreoni, J. (1989). Giving with Impure Altruism: Applications to Charity and Ricardian Equivalence. *Journal of Political Economy*, 97(6):1447–1458.
- Andreoni, J. (1993). An Experimental Test of the Public-Goods Crowding-Out Hypothesis. *American Economic Review*, 83(5):1317–1327.
- Andreoni, J. and Miller, J. (2002). Giving according to GARP: An Experimental Test of the Consistency of Preferences for Altruism. *Econometrica*, 70(2):737–753.
- Atkenson, A. (2020). What Will Be the Economic Impact of COVID-19 in the US? Rough Estimates of Disease Scenarios. *NBER Working Paper No. 26867*.
- Bartik, A. W., Bertrand, M., Cullen, Z. B., Glaeser, E. L., Luca, M., and Stanton, C. T. (2020). How Are Small Businesses Adjusting to COVID-19? Early Evidence from a Survey. *NBER Working Paper No. 26989*.
- Becker, G. (1974). A Theory of Social Interactions. *Journal of Political Economy*, 82(6):1063–1093.
- Berg, J., Dickhaut, J., and McCabe, K. (1995). Trust, Reciprocity, and Social History. *Games and Economic Behavior*, 10(1):122–142.
- Binder, C. (2020). Coronavirus Fears and Macroeconomic Expectations. *Review of Economics & Statistics*. Forthcoming.

- Bloch, F., Géricot, G., and Ray, D. (2008). Informal Insurance in Social Networks. *Journal of Economic Theory*, 143(1):36–58.
- Bohnet, I. and Frey, B. S. (1999). Social Distance and Other-Regarding Behavior in Dictator Games: Comment. *American Economic Review*, 89(1):335–339.
- Bolton, G. E. and Ockenfels, A. (2000). ERC: A Theory of Equity, Reciprocity, and Competition. *American Economic Review*, 90(1):166–193.
- Bramoullé, Y. and Kranton, R. (2007). Risk-Sharing Networks. *Journal of Economic Behavior & Organization*, 64(3-4):275–294.
- Colizza, V., Pastor-Satorras, R., and Vespignani, A. (2007). Reaction–diffusion processes and metapopulation models in heterogeneous networks. *Nature Physics*, 3:276–282.
- Coven, J. and Gupta, A. (2020). Disparities in Mobility Responses to COVID-19. *NYU Stern Working Paper*.
- Currarini, S., Jackson, M. O., and Pin, P. (2009). An Economic Model of Friendship: Homophily, Minorities, and Segregation. *Econometrica*, 77(4):1003–1045.
- Diamond, P. A. (1982). Aggregate Demand Management in Search Equilibrium. *Journal of Political Economy*, 90(5):881–894.
- Durante, R., Guiso, L., and Gulino, G. (2020). Asocial Capital: Civic Culture and Social Distancing during COVID-19. *CEPR Discussion Paper No. 14820-4*.
- Eichenbaum, M., Rebelo, S., and Trabandt, M. (2020). The Macroeconomics of Epidemics. *CEPR Discussion Paper No. 14520*.
- Falk, A., Becker, A., Dohmen, T., Enke, B., Huffman, D., and Sunde, U. (2018). Global Evidence on Economic Preferences. *Quarterly Journal of Economics*, 133(4):1645–1692.
- Falk, A., Becker, A., Dohmen, T., Huffman, D., and Sunde, U. (2016). The Preference Survey Module: A Validated Instrument for Measuring Risk, Time, and Social Preferences. *IZA Discussion Paper No. 9674*.

- Farboodi, M., Jarosch, G., and Shimer, R. (2020). Externality of Social Distancing. *Covid Economics: Vetted and Real-Time Papers*, 9.
- Fehr, E. and Gächter, S. (2000). Fairness and Retaliation: The Economics of Reciprocity. *Journal of Economic Perspectives*, 14(3):159–181.
- Fehr, E. and Schmidt, K. M. (1999). A Theory of Fairness, Competition, and Cooperation. *Quarterly Journal of Economics*, 114(3):817–868.
- Fetzer, T., Hensel, L., Hermle, J., and Roth, C. (2020). Coronavirus Perceptions and Economic Anxiety. *Review of Economics & Statistics*. Forthcoming.
- Garibaldi, P., Moen, E. R., and Pissarides, C. A. (2020). Modelling Contacts and Transitions in the SIR Epidemics Model. *Covid Economics: Vetted and Real-Time Papers*, 5.
- Glaeser, E. L., Gorbach, C. S., and Redding, S. J. (2020). How Much does COVID-19 Increase with Mobility? Evidence from New York and Four Other U.S. Cities. *NBER Working Paper No. 27519*.
- Gonzalez-Eiras, M. and Niepelt, D. (2020). On the Optimal “Lockdown” during an Epidemic. *CESifo Working Paper No. 8240*.
- Goolsbee, A. and Syverson, C. (2020). Fear, Lockdown, and Diversion: Comparing Drivers of Pandemic Economic Decline 2020. *NBER Working Paper No. 27432*.
- Hall, R. E., Jones, C. I., and Klenow, P. J. (2020). Trading Off Consumption and COVID-19 Deaths. *Stanford University Working Paper No. 20-026*.
- Hethcote, H. W. (2000). The Mathematics of Infectious Diseases. *SIAM Review*, 42(4):599–653.
- Jones, C. J., Philippon, T., and Venkateswaran, V. (2020). Optimal Mitigation Policies in a Pandemic: Social Distancing and Working from Home. *NBER Working Paper No. 26984*.
- Keppo, J., Kudlyak, M., Quercioli, E., Smith, L., and Wilson., A. (2020). The Behavioral

- SIR Model, with Applications to the Swine Flu and COVID-19 Pandemics. *University of Wisconsin-Madison Working Paper*.
- Kermack, W. O. and McKendrick, A. G. (1927). A Contribution to the Mathematical Theory of Epidemics. *Proceedings of the Royal Society of London*, 115(772):700–721.
- Kossinets, G. and Watts, D. J. (2009). Origins of Homophily in an Evolving Social Network. *American Journal of Sociology*, 115(2):405–450.
- Moinet, A., Pastor-Satorras, R., and Barrat, A. (2018). Effect of Risk Perception on Epidemic Spreading in Temporal Networks. *Physical Review E*, 97:012313.
- Moser, C. A. and Yared, P. (2020). Pandemic Lockdown: The Role of Government Commitment. *NBER Working Paper No. 27062*.
- Newman, N. (2018). *Networks*. Oxford University Press, 2nd edition.
- Pastor-Satorras, R. and Vespignani, A. (2001a). Epidemic Dynamics and Endemic States in Complex Networks. *Physical Review E*, 63(6):066117.
- Pastor-Satorras, R. and Vespignani, A. (2001b). Epidemic Spreading in Scale-Free Networks. *Physical Review Letters*, 86(14):3200–3203.
- Perra, N., Gonçalves, B., Pastor-Satorras, R., and Vespignani, A. (2012). Activity Driven Modeling of Time Varying Networks. *Scientific Reports*, 2(469).
- Petrongolo, B. and Pissarides, C. A. (2001). Looking into the Black Box: A Survey of the Matching Function. *Journal of Economic Literature*, 39(2):390–431.
- Pissarides, C. A. (2000). *Equilibrium Unemployment Theory*. The MIT Press, 2nd edition.

A. Tables

Table 1
List of Countries in Most Restrictive Sample

Country	Number of cities in different regions
Australia	5
Austria	2
Brazil	7
Canada	6
France	13
Germany	17
India	5
Indonesia	2
Italy	10
Japan	25
Mexico	9
Netherlands	5
Poland	4
Portugal	2
Russia	4
South Africa	2
Spain	4
Sweden	3
Switzerland	4
Turkey	4
United Kingdom	16
United States	111
Vietnam	2

This table lists all countries with at least two cities in different regions that can be matched to the Global Preferences Survey (see Falk et al. (2018)).

Table 2
Summary Statistics

	Country level				City/regional level			
	Mean	Std. dev.	Min	Max	Mean	Std. dev.	Min	Max
Corona ST	23.38	21.86	1.00	100.00	23.54	22.32	0.00	100.00
Stringency index	0.50	0.32	0.00	1.00				
Walking					90.17	44.17	2.43	629.86
Driving					88.11	34.30	5.89	252.00
Transit					69.60	39.32	4.11	360.87
Patience					0.56	0.46	-0.94	1.42
Altruism					0.15	0.34	-2.10	0.76
Neg. reciprocity					0.06	0.27	-1.00	1.03
Trust					0.06	0.33	-1.46	0.85
<i>N</i>	6,953				41,653			

This table presents summary statistics for the main dependent and independent variables, which correspond to the respective descriptions in Tables 3 to 6. The statistics in the first four columns are at the country-day level, whereas the statistics in the last four columns are at the city-day level for the three mobility outcomes (walking, driving, and transit) and at the region-day level for all remaining variables. Furthermore, the sample in the last four columns is limited to countries with at least two cities in different regions.

Table 3
Effect of Fear and Government Responses on Mobility – Country- and Regional-level Variation

Sample Variable	ln(Walking)	ln(Driving)	ln(Transit)	ln(Walking)	ln(Driving)	ln(Transit)
	All countries			Multi-region countries		
	(1)	(2)	(3)	(4)	(5)	(6)
ln(Corona ST _{t-1})	-0.078** (0.030)	-0.089*** (0.025)	-0.087** (0.038)	-0.062** (0.031)	-0.072*** (0.025)	-0.094*** (0.032)
Lockdown	-0.344*** (0.053)	-0.314*** (0.040)	-0.391*** (0.060)	-0.375*** (0.052)	-0.330*** (0.041)	-0.378*** (0.061)
Lifting	0.288*** (0.043)	0.256*** (0.035)	0.348*** (0.055)	0.274*** (0.046)	0.256*** (0.037)	0.367*** (0.063)
Deaths per capita _{t-1}	-0.291 (0.204)	0.186 (0.147)	0.020 (0.215)	-0.416* (0.222)	0.154 (0.165)	-0.063 (0.268)
Cases per capita _{t-1}	0.076*** (0.019)	0.027* (0.014)	-0.053*** (0.020)	0.091*** (0.017)	0.034** (0.013)	-0.055** (0.023)
City FE	Y	Y	Y	Y	Y	Y
Date FE	Y	Y	Y	Y	Y	Y
Adj. R ²	0.77	0.79	0.83	0.77	0.79	0.83
N	45,502	46,608	30,494	40,610	41,242	28,021

The level of observation is the city-date level it , where city i is in region g of country c . In the last three columns, the sample is limited to countries c with at least two cities i in different regions g . The dependent variable in columns 1 and 4 is the natural logarithm of Apple Mobility’s walking index for city i at date t . The dependent variable in columns 2 and 5 is the natural logarithm of Apple Mobility’s driving index for city i at date t . The dependent variable in columns 3 and 6 is the natural logarithm of Apple Mobility’s transit index for city i at date t . In the first three columns, $Corona ST_{ct-1}$ is the Google Trends Index for the search term “Coronavirus” in country c at date $t - 1$. In the last three columns, $Corona ST_{gt-1}$ is the Google Trends Index for the search term “Coronavirus” in region g at date $t - 1$. $Lockdown_{ct}$ is an indicator variable for the entire post-period following a lockdown in country c (or state/region g for the US), and $Lifting_{ct}$ is an indicator variable for the period following the first date which marks the lifting of restrictions in country c (or state/region g for the US). $Deaths per capita_{ct-1}$ and $Cases per capita_{ct-1}$ are, respectively, the number of deaths and infection cases per capita in country c at date $t - 1$, and are multiplied by 1,000. Robust standard errors (double-clustered at the city and date levels) are in parentheses.

Table 4
Effect of Fear and Government Responses on Mobility: The Role of Patience –
Regional-level Variation

Variable	ln(Walking) (1)	ln(Driving) (2)	ln(Transit) (3)	ln(Walking) (4)	ln(Driving) (5)	ln(Transit) (6)
ln(Corona ST _{t-1})	-0.030* (0.016)	-0.029** (0.012)	-0.009 (0.025)	0.038** (0.016)	0.029** (0.012)	0.063*** (0.020)
Lockdown	-0.653*** (0.082)	-0.521*** (0.057)	-0.752*** (0.096)			
Lockdown × Patience	0.423*** (0.085)	0.257*** (0.051)	0.413*** (0.093)			
Lifting	0.206*** (0.042)	0.188*** (0.036)	0.289*** (0.059)			
Lifting × Patience	-0.094* (0.048)	-0.096** (0.040)	-0.182*** (0.062)			
Stringency index				-1.422*** (0.136)	-1.213*** (0.103)	-1.978*** (0.165)
Stringency index × Patience				0.545*** (0.124)	0.277*** (0.062)	0.409*** (0.151)
Deaths per capita _{t-1}	0.515* (0.267)	0.842*** (0.221)	1.367*** (0.292)	0.185 (0.301)	0.588** (0.250)	1.101*** (0.292)
Cases per capita _{t-1}	-0.041** (0.017)	-0.064*** (0.018)	-0.145*** (0.026)	-0.004 (0.022)	-0.036* (0.021)	-0.084*** (0.025)
City FE	Y	Y	Y	Y	Y	Y
Date FE	Y	Y	Y	Y	Y	Y
Country-month FE	Y	Y	Y	Y	Y	Y
Adj. R ²	0.88	0.90	0.90	0.88	0.90	0.91
N	40,610	41,242	28,021	39,100	39,728	26,996

The level of observation is the city-date level it , where city i is in region g of country c . The sample is limited to countries c with at least two cities i in different regions g . The dependent variable in columns 1 and 4 is the natural logarithm of Apple Mobility’s walking index for city i at date t . The dependent variable in columns 2 and 5 is the natural logarithm of Apple Mobility’s driving index for city i at date t . The dependent variable in columns 3 and 6 is the natural logarithm of Apple Mobility’s transit index for city i at date t . $Corona ST_{gt-1}$ is the Google Trends Index for the search term “Coronavirus” in region g at date $t - 1$. $Lockdown_{ct}$ is an indicator variable for the entire post-period following a lockdown in country c (or state/region g for the US), and $Lifting_{ct}$ is an indicator variable for the period following the first date which marks the lifting of restrictions in country c (or state/region g for the US). $Stringency index_{ct}$ is the stringency index (taken from the Oxford COVID-19 Government Response Tracker) from 0 to 1, reflecting the different policy responses that governments have taken, in country c at date t . $Patience_g$ is the average value for the measure of time preference in region g reported by Falk et al. (2018). $Deaths per capita_{ct-1}$ and $Cases per capita_{ct-1}$ are, respectively, the number of deaths and infection cases per capita in country c at date $t - 1$, and are multiplied by 1,000. Robust standard errors (double-clustered at the city and date levels) are in parentheses.

Table 5
Effect of Fear and Government Responses on Mobility: The Role of Negative Reciprocity – Regional-level Variation

Variable	ln(Walking) (1)	ln(Driving) (2)	ln(Transit) (3)	ln(Walking) (4)	ln(Driving) (5)	ln(Transit) (6)
ln(Corona ST _{t-1})	-0.031* (0.016)	-0.032** (0.012)	-0.004 (0.026)	0.034** (0.016)	0.026** (0.012)	0.065*** (0.021)
Lockdown	-0.369*** (0.054)	-0.345*** (0.041)	-0.436*** (0.058)			
Lockdown × Neg. reciprocity	-0.125 (0.113)	-0.177*** (0.067)	-0.185 (0.163)			
Lifting	0.135*** (0.018)	0.118*** (0.016)	0.135*** (0.023)			
Lifting × Neg. reciprocity	0.293*** (0.069)	0.215*** (0.054)	0.326*** (0.104)			
Stringency index				-1.166*** (0.119)	-1.071*** (0.095)	-1.725*** (0.127)
Stringency index × Neg. reciprocity				0.097 (0.164)	-0.053 (0.074)	-0.060 (0.220)
Deaths per capita _{t-1}	0.346 (0.289)	0.743*** (0.227)	1.270*** (0.307)	0.097 (0.329)	0.553** (0.261)	1.084*** (0.303)
Cases per capita _{t-1}	-0.032** (0.015)	-0.058*** (0.017)	-0.144*** (0.025)	0.001 (0.022)	-0.033 (0.021)	-0.087*** (0.026)
City FE	Y	Y	Y	Y	Y	Y
Date FE	Y	Y	Y	Y	Y	Y
Country-month FE	Y	Y	Y	Y	Y	Y
Adj. R ²	0.87	0.90	0.90	0.87	0.90	0.90
N	40,610	41,242	28,021	39,100	39,728	26,996

The level of observation is the city-date level it , where city i is in region g of country c . The sample is limited to countries c with at least two cities i in different regions g . The dependent variable in columns 1 and 4 is the natural logarithm of Apple Mobility’s walking index for city i at date t . The dependent variable in columns 2 and 5 is the natural logarithm of Apple Mobility’s driving index for city i at date t . The dependent variable in columns 3 and 6 is the natural logarithm of Apple Mobility’s transit index for city i at date t . $Corona\ ST_{gt-1}$ is the Google Trends Index for the search term “Coronavirus” in region g at date $t - 1$. $Lockdown_{ct}$ is an indicator variable for the entire post-period following a lockdown in country c (or state/region g for the US), and $Lifting_{ct}$ is an indicator variable for the period following the first date which marks the lifting of restrictions in country c (or state/region g for the US). $Stringency\ index_{ct}$ is the stringency index (taken from the Oxford COVID-19 Government Response Tracker) from 0 to 1, reflecting the different policy responses that governments have taken, in country c at date t . $Neg.\ reciprocity_g$ is the average value for the measure of negative reciprocity in region g reported by Falk et al. (2018). $Deaths\ per\ capita_{ct-1}$ and $Cases\ per\ capita_{ct-1}$ are, respectively, the number of deaths and infection cases per capita in country c at date $t - 1$, and are multiplied by 1,000. Robust standard errors (double-clustered at the city and date levels) are in parentheses.

Table 6
Effect of Fear and Government Responses on Mobility: The Role of Altruism –
Regional-level Variation

Variable	ln(Walking) (1)	ln(Driving) (2)	ln(Transit) (3)	ln(Walking) (4)	ln(Driving) (5)	ln(Transit) (6)
ln(Corona ST _{t-1})	-0.029* (0.016)	-0.029** (0.012)	0.001 (0.026)	0.032* (0.016)	0.026** (0.012)	0.063*** (0.022)
Lockdown	-0.439*** (0.061)	-0.390*** (0.047)	-0.622*** (0.081)			
Lockdown × Altruism	0.274** (0.107)	0.159** (0.075)	0.575*** (0.163)			
Lifting	0.243*** (0.030)	0.186*** (0.025)	0.223*** (0.036)			
Lifting × Altruism	-0.362*** (0.063)	-0.227*** (0.065)	-0.269*** (0.083)			
Stringency index				-1.171*** (0.121)	-1.086*** (0.097)	-1.845*** (0.135)
Stringency index × Altruism				0.176 (0.169)	0.080 (0.081)	0.714*** (0.249)
Deaths per capita _{t-1}	0.446 (0.297)	0.798*** (0.240)	1.354*** (0.297)	0.110 (0.324)	0.549** (0.262)	1.088*** (0.289)
Cases per capita _{t-1}	-0.029* (0.016)	-0.058*** (0.018)	-0.141*** (0.025)	0.002 (0.022)	-0.033 (0.021)	-0.077*** (0.024)
City FE	Y	Y	Y	Y	Y	Y
Date FE	Y	Y	Y	Y	Y	Y
Country-month FE	Y	Y	Y	Y	Y	Y
Adj. R ²	0.87	0.90	0.90	0.87	0.90	0.91
N	40,610	41,242	28,021	39,100	39,728	26,996

The level of observation is the city-date level it , where city i is in region g of country c . The sample is limited to countries c with at least two cities i in different regions g . The dependent variable in columns 1 and 4 is the natural logarithm of Apple Mobility’s walking index for city i at date t . The dependent variable in columns 2 and 5 is the natural logarithm of Apple Mobility’s driving index for city i at date t . The dependent variable in columns 3 and 6 is the natural logarithm of Apple Mobility’s transit index for city i at date t . $Corona ST_{gt-1}$ is the Google Trends Index for the search term “Coronavirus” in region g at date $t - 1$. $Lockdown_{ct}$ is an indicator variable for the entire post-period following a lockdown in country c (or state/region g for the US), and $Lifting_{ct}$ is an indicator variable for the period following the first date which marks the lifting of restrictions in country c (or state/region g for the US). $Stringency index_{ct}$ is the stringency index (taken from the Oxford COVID-19 Government Response Tracker) from 0 to 1, reflecting the different policy responses that governments have taken, in country c at date t . $Altruism_g$ is the average value for the measure of altruism in region g reported by Falk et al. (2018). $Deaths per capita_{ct-1}$ and $Cases per capita_{ct-1}$ are, respectively, the number of deaths and infection cases per capita in country c at date $t - 1$, and are multiplied by 1,000. Robust standard errors (double-clustered at the city and date levels) are in parentheses.

Table 7
Effect of Fear and Government Responses on Mobility: The Role of Trust –
Regional-level Variation

Variable	ln(Walking) (1)	ln(Driving) (2)	ln(Transit) (3)	ln(Walking) (4)	ln(Driving) (5)	ln(Transit) (6)
ln(Corona ST _{t-1})	-0.036** (0.015)	-0.032*** (0.012)	-0.019 (0.024)	0.029* (0.016)	0.025** (0.012)	0.050*** (0.019)
Lockdown	-0.432*** (0.056)	-0.383*** (0.044)	-0.537*** (0.065)			
Lockdown × Trust	0.409*** (0.110)	0.221*** (0.063)	0.505*** (0.128)			
Lifting	0.155*** (0.024)	0.134*** (0.019)	0.160*** (0.029)			
Lifting × Trust	-0.110* (0.066)	-0.094** (0.047)	-0.111** (0.049)			
Stringency index				-1.180*** (0.119)	-1.089*** (0.097)	-1.799*** (0.132)
Stringency index × Trust				0.509*** (0.164)	0.224*** (0.080)	0.633*** (0.185)
Deaths per capita _{t-1}	0.413 (0.297)	0.781*** (0.239)	1.306*** (0.315)	0.117 (0.324)	0.552** (0.262)	1.073*** (0.300)
Cases per capita _{t-1}	-0.036** (0.017)	-0.062*** (0.018)	-0.146*** (0.026)	0.003 (0.022)	-0.032 (0.021)	-0.081*** (0.025)
City FE	Y	Y	Y	Y	Y	Y
Date FE	Y	Y	Y	Y	Y	Y
Country-month FE	Y	Y	Y	Y	Y	Y
Adj. R ²	0.87	0.90	0.90	0.87	0.90	0.91
N	40,610	41,242	28,021	39,100	39,728	26,996

The level of observation is the city-date level it , where city i is in region g of country c . The sample is limited to countries c with at least two cities i in different regions g . The dependent variable in columns 1 and 4 is the natural logarithm of Apple Mobility’s walking index for city i at date t . The dependent variable in columns 2 and 5 is the natural logarithm of Apple Mobility’s driving index for city i at date t . The dependent variable in columns 3 and 6 is the natural logarithm of Apple Mobility’s transit index for city i at date t . $Corona ST_{gt-1}$ is the Google Trends Index for the search term “Coronavirus” in region g at date $t - 1$. $Lockdown_{ct}$ is an indicator variable for the entire post-period following a lockdown in country c (or state/region g for the US), and $Lifting_{ct}$ is an indicator variable for the period following the first date which marks the lifting of restrictions in country c (or state/region g for the US). $Stringency index_{ct}$ is the stringency index (taken from the Oxford COVID-19 Government Response Tracker) from 0 to 1, reflecting the different policy responses that governments have taken, in country c at date t . $Trust_g$ is the average value for the measure of trust in region g reported by Falk et al. (2018). $Deaths per capita_{ct-1}$ and $Cases per capita_{ct-1}$ are, respectively, the number of deaths and infection cases per capita in country c at date $t - 1$, and are multiplied by 1,000. Robust standard errors (double-clustered at the city and date levels) are in parentheses.

B. First-Order Conditions of the Social Planner in the Homogeneous SIR Model

The first-order conditions for the social planner's problem in Definition 3 for the home activity of infected and susceptible individuals and for the home and outside activities of recovered individuals are equivalent to the ones obtained under the decentralized equilibrium. For the social activity of susceptible and infected individuals, however, we have:

$$\frac{\partial U(x_{h,t}^S, x_{s,t}^S)}{\partial x_{s,t}^S} + \beta \frac{\partial p_t^P(\cdot)}{\partial x_{s,t}^S} [(\hat{V}_{t+1}^I - \hat{V}_{t+1}^S)] + \beta(1 - p_t^P(\cdot)) \left[\frac{\partial \hat{V}_{t+1}^S}{\partial S_{t+1}} \frac{\partial S_{t+1}}{\partial x_{s,t}^S} + \frac{\partial \hat{V}_{t+1}^S}{\partial I_{t+1}} \frac{\partial I_{t+1}}{\partial x_{s,t}^S} \right] = 0 \quad (55)$$

$$\frac{\partial U(x_{h,t}^I, x_{s,t}^I)}{\partial x_{s,t}^I} + \delta \left\{ \beta \frac{\partial p_t^P(\cdot)}{\partial x_{s,t}^I} [(\hat{V}_{t+1}^I - \hat{V}_{t+1}^S)] + \beta(1 - p_t^P(\cdot)) \left[\frac{\partial \hat{V}_{t+1}^S}{\partial S_{t+1}} \frac{\partial S_{t+1}}{\partial x_{s,t}^I} + \frac{\partial \hat{V}_{t+1}^S}{\partial I_{t+1}} \frac{\partial I_{t+1}}{\partial x_{s,t}^I} \right] \right\} = 0. \quad (56)$$

C. First-Order Conditions of the Social Planner in the SIR-Network Model

The first-order conditions for the social planner's problem in Definition 4 for the home activity of infected and susceptible individuals and for the home and outside activities of recovered individuals are equivalent to the ones obtained under the decentralized equilibrium. For the social activity of susceptible and infected individuals in each group j , however, the first-order conditions are as follows:

$$\frac{\partial U(x_{h,t}^{S,j}, x_{s,t}^{S,j})}{\partial x_{s,t}^{S,j}} + \beta \frac{\partial p^{Pj}(\cdot)}{\partial x_{s,t}^{S,j}} [\hat{V}_{t+1}^{I,j} - \hat{V}_{t+1}^{S,j}] + \beta(1 - p_t^{Pj}(\cdot)) \sum_k \left[\frac{\partial \hat{V}_{t+1}^{S,j}}{\partial S_{t+1}^k} \frac{\partial S_{t+1}^k}{\partial x_{s,t}^{S,j}} + \frac{\partial \hat{V}_{t+1}^{S,j}}{\partial I_{t+1}^k} \frac{\partial I_{t+1}^k}{\partial x_{s,t}^{S,j}} \right] = 0 \quad (57)$$

$$\frac{\partial U(x_{h,t}^{I,j}, x_{s,t}^{I,j})}{\partial x_{s,t}^{I,j}} + \delta \beta \sum_k \left\{ \frac{\partial p^{Pk}(\cdot)}{\partial x_{s,t}^{I,j}} [(\hat{V}_{t+1}^{I,k} - \hat{V}_{t+1}^{S,k})] + (1 - p_t^{Pk}(\cdot)) \sum_n \left[\frac{\partial \hat{V}_{t+1}^{S,k}}{\partial S_{t+1}^n} \frac{\partial S_{t+1}^n}{\partial x_{s,t}^{I,j}} + \frac{\partial \hat{V}_{t+1}^{S,k}}{\partial I_{t+1}^n} \frac{\partial I_{t+1}^n}{\partial x_{s,t}^{I,j}} \right] \right\} = 0. \quad (58)$$